

**CHARACTERIZATION OF FRACTURE DAMAGE ZONES IN THE ABIQUIU
FORMATION, PLAZA BLANCA, NEW MEXICO**

A Thesis Presented to
the Faculty of the Department of Earth and Atmospheric Sciences
University of Houston

In Partial Fulfillment
of the Requirements for the Degree
Master of Science

By
Ross Anthony Andrea
May 2017

**CHARACTERIZATION OF FRACTURE DAMAGE ZONES IN THE
ABIQUIU FORMATION, PLAZA BLANCA, NEW MEXICO**

Ross Anthony Andrea

APPROVED:

Dr. Michael A. Murphy, Chairman

Dr. Shuhab Khan

Dr. Jim DeGraff

**Dr. Dan E. Wells
Dean, College of Natural Science and
Mathematics**

ACKNOWLEDGEMENTS

Richelle Hepler is the corner stone of this project. Her unwavering support is the foundation of my motivation. Words cannot describe how much you mean to me.

This project would not be possible without the inspiration and confidence of Dr. Yiduo Liu. He is a true friend and mentor. His creative and dedicated scientific mind is rooted in the fundamentals of geology and scientific discovery. I cherish all our discussions and times in the field. I give the upmost gratitude to Dr. Mike Murphy for allowing me the freedom to explore, discover, and enjoy geology while providing invaluable lessons in the field, in the classroom, in life. It is truly an honor to have been part of his research group. Dr. Jim DeGraff was always enthusiastic to discuss the finer points of the project, no matter what strange turn it took. He was there from the beginning providing insight to fundamental structural geology concepts that kept the project grounded. Dr. Shuhab Khan for suggesting the use of Gigapan imagery as a way to make a large project feasible and giving that “tough love” necessary to step outside of my comfort zone and learn new methods for approaching geology. Dr. Jinny Sisson provided the Gigapan camera on short notice. Erik Fischer provided air transportation, a warm place to stay, and endless laughs. Dr. Joel Saylor taught me how to measure section and organized the best geology field trips to New Mexico. A special thanks to Jennitta Andrea. She seems to always be there when I need someone the most. I also thank my ever loving mother, Dr. Bernadette Andrea, for setting the bar of intellectual knowledge so high and my stepfather, Dr. Ben Olguin for emphasizing critical thinking early on. Thanks to all the residents of the Plaza Blanca Land Grant for letting me study geology on your land. A final acknowledgement to all my friends and colleagues not mentioned above . Thank you.

**CHARACTERIZATION OF FRACTURE DAMAGE ZONES IN THE ABIQUIU
FORMATION, PLAZA BLANCA, NEW MEXICO**

An Abstract of a Thesis
Presented to
the Faculty of the Department of Earth and Atmospheric Sciences
University of Houston

In Partial Fulfillment
of the Requirements for the Degree
Master of Science

By
Ross Anthony Andrea
May 2017

ABSTRACT

The methods used for characterizing fracture damage-zones in the Plaza Blanca, New Mexico region yielded a data-rich study. New concepts such as a “splay zone” are introduced to help explain a complex accommodation zone formed by hard linked SE-dipping normal faults called the Plaza Blanca Fault (PBF) splay. These faults are part of a broader connected fault system within the Rio Grande Rift. The total extension in the Plaza Blanca region is ~5.8% with ~290 meters of E-W horizontal extension. The throw across this region exceeds the throw of the rift-bounding Cañones fault. The width of the PBF damage zone vs fault throw is consistent with previous studies. Sampling techniques at the PBF provided fracture information in three dimensions at various locations and at scales ranging from micrometer to kilometer. A 2 m-diameter circular window is used in the field to sample fracture populations on bedding planes. Fracture density, scale, and geometry vary with respect fault core proximity. At this fault splay the damage zone becomes more complicated as two major faults interact. Several observations about fracture density are made from the sample windows: fracture density in the damage zone increases with proximity to the fault core, fracture density is highest at the fault core and splay point, the higher the fracture density the smaller the fracture length per area, and the more fractures per area the more irregular the fracture orientation. Basic connectivity is a factor in understanding potential transmissivity through a network. Identifying three fundamental connective facets (I, X, Y) are part of the window analysis. These connective facets are then plotted on a ternary diagram where connections per branch (C_B) can be quantified. The higher fracture density, the more connected the network is. There is a quasi-linear correlation between the sum of connective facets versus the fracture density per window. Using a Gigapan image of the PBF, nearly 30,000 fractures are annotated. This detailed annotation provides geometry, density, and connectivity at a high resolution. These methods, and others, enhance the understanding of how permeability is affected by fracture damage zones.

TABLE OF CONTENTS

1. INTRODUCTION..... 1

1.1 Fault Components..... 1

1.2 Project Overview..... 4

2. GEOLOGIC BACKGROUND..... 7

2.1 Tectonic History..... 7

2.1.1 Proterozoic Shortening..... 7

2.1.2 Ancestral Rocky Mountains..... 7

2.1.3 Laramide Shortening..... 7

2.1.4 Rio Grande Rift Extension..... 8

2.2 Regional Stratigraphy..... 9

2.2.1 Paleozoic..... 9

2.2.2 Triassic..... 9

2.2.3 Jurassic..... 10

2.2.4 Cenozoic..... 10

3. PLAZA BLANCA GEOLOGY..... 16

3.1 Field Investigation..... 18

3.1.1 Bedding..... 18

3.1.2 Faulting..... 18

3.1.3 Outcrop Observations..... 19

3.2 Geologic Mapping..... 21

3.3 Cross Sections..... 21

3.4 Detailed Stratigraphy..... 22

3.4.1 Measured Stratigraphic Sections..... 23

4. METHODS..... 26

4.1 Regional..... 26

4.2 Fracture Circles..... 26

4.3 Gigapan Imagery..... 30

4.4 Thin Sections..... 34

5. RESULTS..... 35

5.1 Throw..... 36

5.2 Microstructures..... 38

5.3 Width of the Plaza Blanca Fault Damage Zone..... 41

5.4 Fracture Characterization	44
5.4.1 Fracture Mechanisms	45
5.4.2 Fracture Geometry	47
5.4.3 Fracture Density	52
5.4.4 Connectivity	54
6. CONCLUSIONS	58
7. FUTURE WORK	60
9. REFERENCES	62

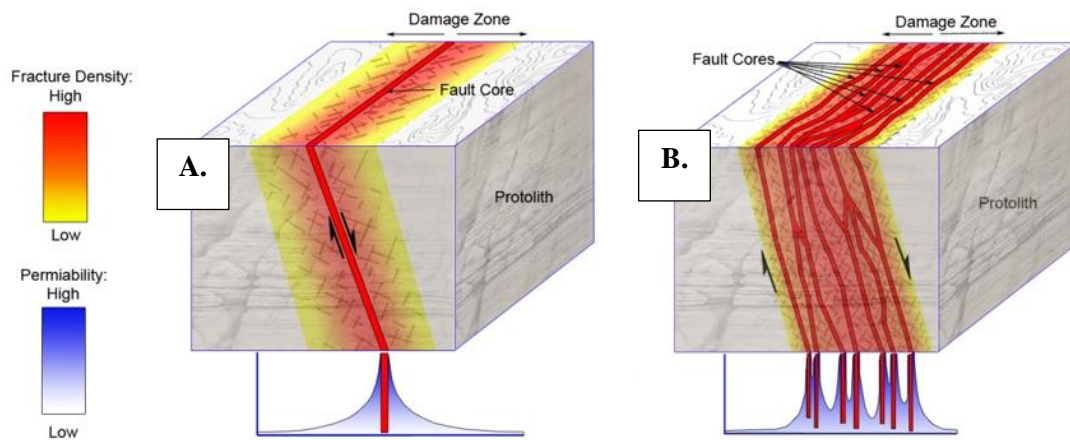
1. INTRODUCTION

1.1 Fault Components

Faults can be divided into four basic components: the protolith or undamaged bedrock, a background damage zone that exhibits minor deformation, a damage zone that has a high density of fractures that form during fault slip and propagation, and the fault core which includes the kinematic slip surface and a narrow zone of low permeability cataclasite. The fault damage zone is the region of fractured rock enveloping the fault core. Field studies show that fracture densities decrease with distance from the fault core (Chester et al., 2005; Mitchell and Faulkner, 2009; Savage and Brodsky, 2011). Observations also show that the width of damage zones increases with displacement. Many factors have been shown to influence fracture-density patterns, including: fractured layer thickness and lithology, bed flexure (Jamison and Stearns, 1982), depth of faulting, and fault plane geometry. However, the observation that damage-zone width increases with displacement suggests that processes such as fault propagation and linkage are first-order controls on damage-zone width. Several studies have investigated this and highlight the importance of progressive strain localization between overlapping fault segments (Peacock, 2002; Kim et al., 2004; Okubo et al., 2005; Childs et al., 2009). This general process involves the development of fractured rock between the overlapping faults referred to as an accommodation or relay zone (Dawers and Anders, 1994; Peacock and Sanderson, 1994; Walsh et al., 1999). As faults propagate and link the accommodation zone is faulted and translated along the linked fault (Cartwright and Mansfield, 1998). How the accommodation zone is beheaded and incorporated into the fault zone is investigated by Childs et al. (2009).

Damage zones fractures are known to increase in density with proximity to the fault core. This simple model (Figure 1.1 A.) depicts how density is related to permeability. The fault core is nearly impermeable due to grain-size reduction, poor sorting, and an abundance of clay minerals.

Multiple fault cores interact in a complex fault system (Figure 1.1 B.), creating a wider damage zone and thus a wider zone of permeability. Conversely, though, a zone of linked faults may produce enhanced zones of fracture density heterogeneity as well as compartmentalizing permeability with bounded impermeable fault cores (Watkins et al., 2015). Although a number of previous studies have quantitatively examined the relationship between damage zone width and fault throw with models of complex fault patterns and associated damage zones across a single fault, fracture networks in a two fault system, which is a very common structure in many prolific basins such as the North Sea and Gulf of Mexico, is still schematic and in need of a more quantitative study (Fossen et al., 2005; Faulkner et al., 2010).



Modified from Faulkner et al. 2010

Figure 1.1: This simple model (A.) depicts how density is related to permeability. The fault core is nearly impermeable due to grain size reduction, poor sorting, and an abundance of clay minerals. Multiple fault cores interact (B.) creating a wider damage zone and thus a wider zone of permeability. Conversely, though, a zone of linked faults may produce enhanced zones of fracture density heterogeneity as well as compartmentalizing permeability with bounded impermeable fault cores.

1.2 Project Overview

The town of Abiquiu is located on the south bank of the Chama River in north central New Mexico. The white cliffs nearby are made famous through the artistic hand of modern painter Georgia O'Keeffe and are aptly named the Abiquiu Formation. Unbeknownst to most who casually pass through, the Abiquiu Formation exhibits more than mere aesthetic beauty. To the trained eye of a geologist, faults and fractures break up what appears to be seemingly subhorizontal, laterally continuous, meter-scale bedding of a relatively homogenous composition and texture. This detailed study aims to characterize the fracture-damage zones within of the Abiquiu Formation that result from the Rio Grande extension. The implications of such a study involve furthering the understanding of geometric and connective relationships in a reservoir rock controlled by interconnected extensional faults. Techniques used in this study to quantify fracture patterns in the damage zones surrounding normal faults are novel and reproducible. The two-part focus of this study is to quantify scaling relationships and characterize connective properties of the fracture networks. These fracture networks relate to connected normal faults in the Plaza Blanca Land Grant region north of the town of Abiquiu, NM.

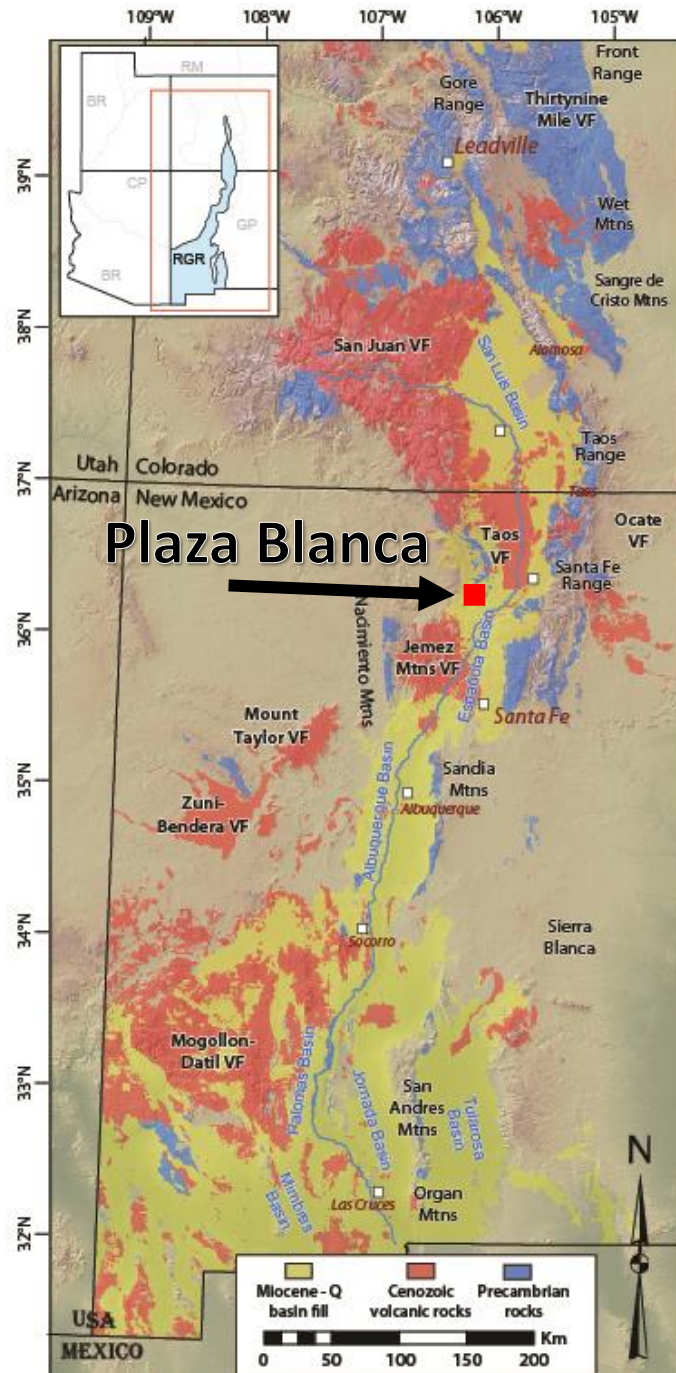
The primary study area features a normal fault splay. The Plaza Blanca fault splays into two SE-dipping, synthetic normal faults. Several studies attribute increased damage zone width and decreased fracture density from the fault core to the magnitude of fault throw. At this fault splay the damage zone is more complex where the two splay faults intersect and interact. This interaction is exhibited in both outcrop along 40 m-high cliffs as well as exposed on the rock in map view. This unique three-dimensional view lends itself to the use of a variety of data collection techniques for the purpose of detailed fracture assessment.

To determine various characteristics of fracture networks in the damage zone and background damage in the splay zone two novel methods are utilized. First we employ a 2 m-diameter

circular-window method and measure fracture orientations, lengths, apertures and connective facets to determine fracture variation along and across the splay zone. Second, a high-resolution Gigapan image is taken to allow for fracture annotation on the outcrop. This technique is critical for assessing fracture network characterization where tactile measurements cannot be obtained on the steep the faces.

Several measured sections are constructed at key locations in order to estimate the throw across the fault zone. This is especially critical due to the seemingly homogenous appearance of the Oligo-Miocene Abiquiu Formation. Detailed field mapping of the Plaza Blanca Fault and surrounding faults provide the extent of the larger fault zone as it relates to the Cañones Fault which is the major rift bounding fault proximal to the region.

This study of the Plaza Blanca Fault provides understanding of the fault/fracture interactions as they relate to fracture scale as well as proximity to the fault. Fracture density provides important information about fluid and pressure interactions in reservoir rocks where normal faults may be present. A detailed look at the damage zone in this field-based study is at a higher resolution than seismic studies and thus may allow for further value in interpreting such fracture-damage zones with low-resolution imagery.



Modified from Ricketts et al., 2015

Figure 1.2: A regional map depicting the extent of the Rio Grande Rift and associated major features. The study area is located within the Abiquiu Embayment within the rift near the western flank in the north-central portion of New Mexico.

2. GEOLOGIC BACKGROUND

2.1 Tectonic History

The study area is located within the Rio Grande Rift near a western boundary. This region has prolonged and complicated tectonic history as far back as the Proterozoic (Figure 1.2).

2.1.1 Proterozoic Shortening

The earliest crustal-shortening event recorded in this region is represented in the heavily deformed Proterozoic crystalline basement rocks in northern and central New Mexico and southern Colorado. Basement rocks in the Tusas Mountains are a result of the Mazatzal and Yavapai orogenic belts and subsequent tectonic events at approximately 1.4 Ga (Aronoff et al., 2016; Williams et al., 1999). A suite of diverse metamorphic rock represents this ancient uplift and acts as one of the topographically high regions bounding the current Rio Grande Rift (e.g., Amato et al., 2008; Daniel et al., 2013; Karlstrom et al., 1997; Whitmeyer and Karlstrom, 2007; Williams, 1991).

2.1.2 Ancestral Rocky Mountains

The second crustal-shortening event is the Ancestral Rocky Mountain orogeny during the late Paleozoic (Kluth, 1986; Ye et al., 1996). Although the tectonic evolution and mechanism are still enigmatic for this orogeny, it is widely suggested that the Ancestral Rocky reactivated the Proterozoic structures (Ye et al., 1996).

2.1.3 Laramide Shortening

The latest shortening event is the Laramide orogeny during the Late Cretaceous to Eocene when the Farallon plate subducted beneath North America (Bird, 1988; Liu et al., 2010; Yonkee and Weil, 2015). This flat-slab subduction was the driving mechanism for the Laramide Orogeny

which lasted approximately 40 million years depending on geographic location (Copeland et al., 2017). As with the Ancestral Rocky Mountains the Laramide-related thrusts took advantage of pre-existing crustal weaknesses. The deep basement-seated thrusts are responsible for the Sangre de Cristo, Brazos-Tusas, Nacimiento, and Picuris Mountains (Cather et al., 2006; Erslev, 2001; Yin and Ingersoll, 1997).

2.1.4 Rio Grande Rift Extension

Following the cessation of the Laramide shortening, Rio Grande rift extension began (Baldrige et al., 1994; Livaccari, 1991) by taking advantage of the weaknesses in the previous shortening structures a continental rift began to separate the Colorado Plateau in the west from the North American Craton (Cather, 1994b). It has been speculated that the Rio Grande extension initiated during the late Oligocene to earliest Miocene (Morgan et al., 1986; Ricketts et al., 2016) and a commonly-held hypothesis is that once the subducted Farallon plate detached from the North American plate a mantle upwelling thinned and weakened the lithosphere and thus initiated the rift (Copeland et al., 2017; Humphreys, 1995).

The Rio Grande Rift spans central and southern Colorado, New Mexico, West Texas, and Chihuahua, Mexico. It separates the Colorado Plateau to the west from the Great Plain to the east. Its northern portion is characterized by three N-trending, narrow, asymmetric axial basins (the San Luis, Espanola, and Albuquerque basins), bounded by basement uplifts (the Sangre de Cristo, Tusas, Nacimiento, and Sandia mountains). These axial basins are surrounded by a series of shallow basins, including the Abiquiu, Culebra, Santa Fe, and Hagan basins/embayments, and separated by two accommodation/transfer zones (the Embudo and Santo Domingo).

The Cañones fault zone is the western boundary of the Abiquiu embayment, and is rooted into a Laramide monocline where a blind thrust has been reactivated (Liu and Murphy, 2013). This region is proximal to the primary study area (Figure 2.2) and is the dominant structural feature.

2.2 Regional Stratigraphy

The generalized stratigraphy of the region includes stratigraphy from the Mesozoic and upper Paleozoic. There is a large disconformity between the Mesozoic strata and the Cenozoic strata. The resulting stratigraphy in the Cañones and Plaza Blanca region lacks a Cretaceous package of strata. The following is a brief description of the geologic formations surrounding the mapping area.

2.2.1 Paleozoic

The Permian Cutler formation is exposed on the foot wall of the Cañones fault and underlies the more prominent Triassic Chinle. It is primarily a slope-forming unit with more weather resistant channels of trough-cross bedded arkosic sand stone often exposed (Kempster et al., 2007).

2.2.2 Triassic

The Chinle Group consists of three members that have a ~200 m total thickness. The lower member is a slope-forming earthy red siltstone to fine grained sandstone (Lucas et. al. 1993). A prominent cliff-forming red-brown laminated sandstone overlies the lower slope-forming member. The two upper members of the Chinle are exposed in the footwall of the Cañones fault while the uppermost member is located in the hanging wall. The uppermost member is composed of a red-brown mudstone and is exposed below the overlying Entrada sandstone and separated by a disconformity (Kelly et. al. 2005).

2.2.3 Jurassic

Several Jurassic formations are exposed in the hanging wall of Cañones Fault.

The Entrada Formation forms cliffs that are 60 m-high with a red base, pink middle, and yellow top composed of fine-to-medium-grained well-sorted quartzarenite eolian sandstone. (Kempster et al., 2007). It is moderately indurated and displays large dune scale trough-cross bedding, ripples, and deformation bands (Kelly et. al. 2005).

The Todilto Formation disconformably overlies the Entrada sand stone. It is a 5 meter thick non-marine limestone with a high organic content and millimeter scale laminations at the base and small folds near the top (Berglof, 2003).

The Morrison Formation disconformably overlies the Todilto limestone. It is a 40-70 meter thick package of green to reddish mudstone with a basal trough-cross bedded channel sandstone (Kelly et. al. 2005).

2.2.4 Cenozoic

There is a large amount of Cretaceous stratigraphy missing beneath the Cenozoic stratigraphy, presumably due to uplift during the Laramide orogeny.

2.2.4.1 El Rito Formation

The El Rito Formation is a thick conglomeratic package of rock. A basal conglomerate is composed of 1 m-clasts of Proterozoic quartzite, schist, and gneiss. The package then normally grades to amalgamated conglomeratic channels with clasts ranging from pebble-to-cobble sized and cemented in a red silt to sand sized micaceous matrix with channels comprised of more sand-sized grains (Kelly et. al. 2005). The El Rito is interpreted by Smith et al., (*in progress*) to have been deposited during the Laramide orogeny. It overlies the Jurassic strata with a large erosional

contact. There is evidence of a large El Rito filled paleo-valley in the north western part of the mapping area that cuts down to the Chinle Group (Smith et al., *in progress*)

2.2.4.2 Ritito Formation

The Ritito Formation lies slightly unconformably above the El Rito Formation with a subtle dip change of 5-10°. It is thought to be related to early onset Rio Grande Rifting (Vazzana and Ingersoll, 1981). It was initially considered the basal conglomerate of the Abiquiu Formation but was later reclassified due to major differences in lithology and provenance (Smith, 1938; Church and Hack, 1939, Maldonado and Kelley, 2009). The Ritito Conglomerate is composed of Proterozoic quartzite and granite subrounded to subangular pebble to cobble-sized clasts with local boulder clasts throughout and cemented in a pinkish sand matrix. Clast composition and paleoflow direction in the Ritito Formation are similar to that of the underlying El Rito Formation (Hamilton, 2009). It is possible that during the Laramide active basins filling with El Rito sediments were also the same basins later filling with the syn-rift Ritito Formation. This may suggest the slight change in dip in the Ritito and El Rito signals the initiation of the Rio Grande Rift. The Ritito Formation is preserved at high elevations in some locations which suggest that these former basins are on the rift shoulder and were inverted rather than down dropped in the rift. (O'Keefe, 2014)

2.2.4.3 Abiquiu Formation

The Abiquiu formation ranges from the late Oligocene to the middle Miocene. This volcanoclastic formation is the result of terrigenous depositional processes including unconfined sheet flow deposits interrupted by meandering channel systems. The sources of volcanic material are from two primary volcanic fields: the San Juan Field to the NW and the Latir Field to the NE. The total thickness of the Abiquiu Formation is approximately 200 m thick and is composed of

several intervals of subtle compositional and sedimentary facies changes (Smith, 1995). A more detailed description is found below.

2.2.4.4 Tesuque Formation

This is the lower member of the Santa Fe Group and overlies the Abiquiu Formation. The entire Santa Fe Group is between 200 and 600 m thick. The lower member of the Tesuque is primarily unconsolidated sandstone with channels composed of tuffaceous fill and fluvial sediment.

***Side note on the Cerrito Blanca**

The Cerrito Blanca has previously been interpreted as part of the Colorado Plateau that has travelled along a basal detachment fault (Maldonado 2008). This is based on evidence of low angle slicken lines at the base of this cliff forming feature within the Tesuque formation. Upon further mapping I have a new interpretation for this Cerrito Blanca feature (Ttoc in Figure 2.2). There appears to be a confluence of connected faults at this location forming a large fault splay. The rock of the Cerrito Blanca is heavily fractured, exhibiting fracture densities similar to that of a fault core or splay point. Furthermore the amount of bedding rotation is significant suggesting synthetic listric faulting as the mechanism of rotation. If this listric rotation is significant and narrow enough it may explain the low angle kinematic indicators. Similar to the fault cores in the Plaza Blanca region, there seems to be an oxidized cementation that renders the Cerrito Blanca more resistant than the surrounding low indurated sandstone. The clasts of the Cerrito Blanca are larger also suggesting the possibility that this is not a large far travelled block from the Colorado Plateau but rather a large channel, possibly a paleo Chama River, that has been heavily faulted, cemented, and rendered more resistant to weathering. Further investigation is required.

2.2.4.5 Magmatism

A continuous Rio Grande Rift extension coincides with periods of episodic volcanism. The study area has several local topographic highs preserved by the Lobato Basalt flows. The Sierra Negra peak (8052 ft) is capped by a basalt flow dated at 5 Ma (Baldrige et al, 1980) and has preserved the upper-most portion of the Abiquiu Formation suggesting local magmatism post Abiquiu deposition and faulting. It is important to note that the basalt flows take advantage of paleo topographic lows and although they represent the current topographic highs it was not the case during deposition. This suggest a large amount of erosion since deposition and possible offset due to faulting. There are several volcanic fields and intrusive basaltic dikes and sills that have been dated. The Canon de Cobre dike is dated at 10 Ma using potassium-argon method and thought to have taken advantage of existing faults separating the El Rito formation and the Abiquiu formation. (Baldrige et al ,1980). Other dikes in the region have been dated at 20 Ma (Maldonado et al., 2013). The dikes in the northwestern margin of the Plaza Blanca field area show small offset suggesting the maximum age of faulting in the Plaza Blanca region is less than 10 Ma. This observation was made from field mapping as well as previous observations by Maldonado et al. (2013). If these relationships are correct it suggests a range of faulting in the Plaza Blanca region between 5 Ma and potentially 20 Ma. If the Lobato basalt flows are faulted there may be evidence that the faulting may be even younger than 5 Ma and potentially active.

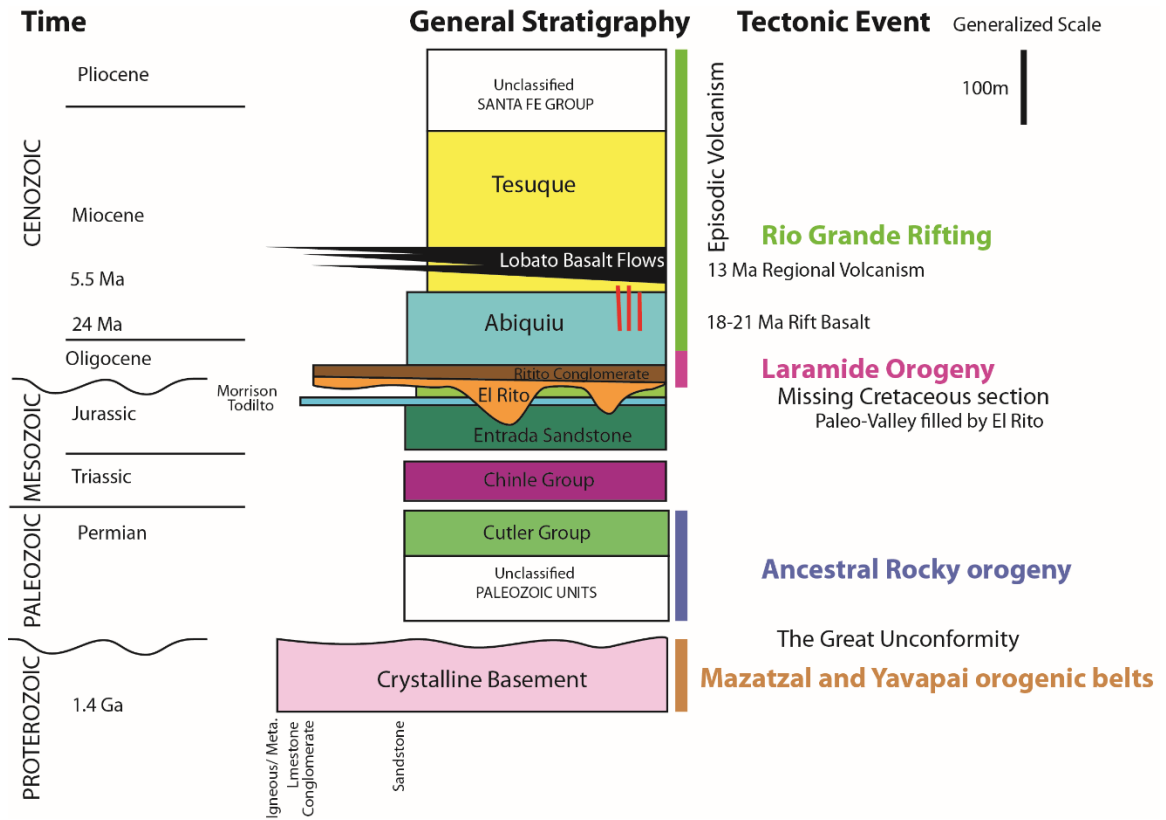


Figure 2: A generalized stratigraphic column of the region showing three major shortening events and the major Rio Grande Rift Extension and igneous events. Notice how the Cretaceous stratigraphy is missing. This might be because of activity during the Laramide orogeny.

3. PLAZA BLANCA GEOLOGY

The study area is located in the Plaza Blanca Land Grant near the Chama River in the Abiquiu Embayment, north-central New Mexico. The rift is bounded by Laramide-age uplifts and more-recent normal faults that extend the rift in an east-west direction. The normal faults that bound the Rio Grande Rift dip toward the rift and are typically accompanied by smaller synthetic faults in the rift fill, which create tilted half grabens. The major bounding fault proximal to Plaza Blanca is the Cañones fault to the northwest (see Figure 2.2). The Cañones fault is a northeast-striking normal fault dipping 75° to the south east and has a throw of approximately 200 m (Baldrige et al., 1994).

The Plaza Blanca region is a three-square-mile region in which the Abiquiu formation is expressed. The western region exposes the Ritito Conglomerate as well as several intrusive basaltic dikes striking NE. These dikes are heavily deformed in some regions and often follow strike of the major faults in the region suggesting they are synrift features that take advantage of fault weaknesses. Normal faults separate the Ritito and the Abiquiu formations and even offset the dikes in certain regions. This suggests the faults are younger than the dikes even if it is not by much. This means the faults are younger than 18 Ma, which is the presumed age of the dikes in this region (Maldonado 2009, Baldrige 1980). In the Abiquiu formation faults and fractures are well preserved both in outcrop and map view. There are many examples of meter scale faults linking, forming Riedel shear geometries, and exhibiting typical damage zone widening environments. These small features are examples within the broader damage zone of one large normal fault in this region. The large fault that extends through the region is called the Plaza Blanca Fault. The fault is exposed in several regions as a fin of oxidized cemented fault core. The attitude of the Plaza Blanca Fault is N50E, 65SE and exhibits dip-slip kinematic motion. This fault links or splays to other faults in several locations and is the main focus of the detailed

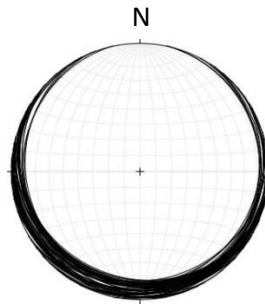
fracture study. The eastern map region exposes the Tesuque formation which overlies the Abiquiu conformably in some areas but is offset slightly in other areas. In the northeast corner of the map area, the Sierra Negra peak is capped by the Lobato basalt flow, which overlies a small portion of exposed Tesuque formation and preserves a large section of the Abiquiu Formation.

3.1 Field Investigation

This study focuses heavily on field observations. The combination of traditional geologic field methods with novel methods allows for a fresh take on how certain low-budget technologies can be applied to geologic field studies.

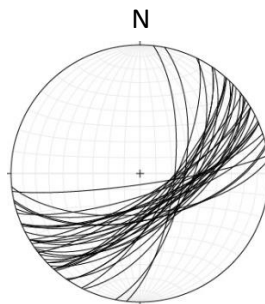
3.1.1 Bedding

Bedding orientations at the Plaza Blanca region are shallowly homoclinally dipping. Below is a lower-hemisphere equal area stereonet that shows 59 bed-plane measurements from the Plaza Blanca region.



3.1.2 Faulting

The faulting in the Plaza Blanca region are dip slip normal faults with an approximate attitude of N55E, 65SE. The stereonet below shows 41 different fault planes in the Plaza Blanca Region. Rakes on the fault surfaces are between 80E and 80W, indicating almost pure dip-slip kinematic motion on these faults.



3.1.3 Outcrop Observations

Initial outcrop observations of the faults and associated fractures in the Abiquiu formation sparked an interest in a more-detailed investigation. The cliffs at the Plaza Blanca region exhibit unvegetated exposures to preserved fault cores, fractures, and stratigraphy. Figure 3.1.3 A. shows a wide-angle view of the Plaza Blanca Fault Splay looking NE. Notice the two prominent fault cores synthetically dipping and converging toward the camera. Figure 3.1.3 B. is an example of a Plaza Blanca fault core preserved in a fin jutting out of the surface. Notice a highly fractured region in the back ground. This is the damaged splay zone on the western splay of the Plaza Blanca Fault. Figure 3.1.3 C. is a cliff in the Abiquiu Formation showing how prominent the fractures are in outcrop. Figure 3.1.3 D. is a meter-scale example of two small faults “soft linking” through an accommodation zone of fractures. Eventually these types of fractures will be swept into a larger damage zone. Unlike the rift bounding Cañones fault (Figure 1 and Figure 2.2), the many faults and fracture damage zones available do not have a significant amount of throw on any single fault (see section 5.1 and Figure 3.2).



Figure 3.1.3 A.:

This is a wide angle view of the Plaza Blanca Fault Splay looking NE. Notice the two prominent fault cores synthetically dipping and converging toward the camera.



Figure 3.1.3 B.:

This is an example of a fin of Plaza Blanca fault core preserved. Notice a highly fractured region in the back ground. This is the damaged splay zone on the western splay of the Plaza Blanca Fault.



Figure 3.1.3 C.:

This is an image of a cliff in the Abiquiu Formation displaying prominent the fractures in outcrop. Notice how difficult it is to determine fault offset due to the stratigraphic difficulties of the Abiquiu Formation.

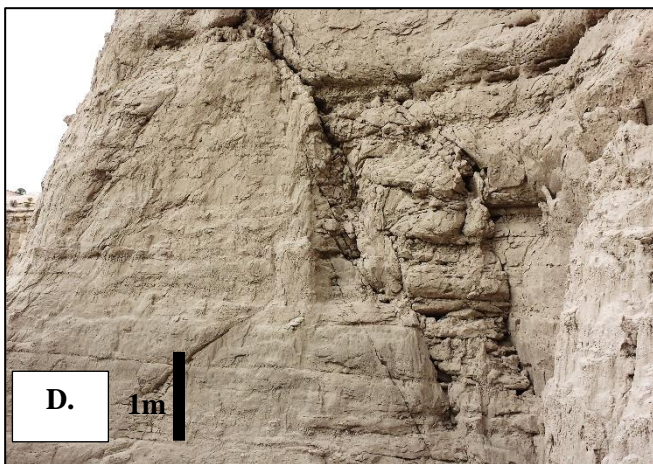


Figure 3.1.3 D.:

Here is a meter-scale example of two small faults “soft linking” through an accommodation zone of fractures. Eventually these types of fractures will be swept into a larger damage zone. Notice the fracture density in the accommodation zone.

3.2 Geologic Mapping

The purpose for constructing a geologic map (Figure 3.2 A.) is to determine geometry and pattern of faulting, determine cross cutting relationships, construct a detailed cross section and build a regional context involving the nearest bounding fault, the Cañones fault.

3.3 Cross Sections

The cross section of the Abiquiu, NM region (Figure 3.2 B.) shows that each fault accommodates a small amount of throw across the entire region. Regional extension of ~5.8% and ~290m of E-W horizontal extension is calculated by measuring the segments of the Ritito in the cross section and applying the extension equation. *Equation 3.3:*

$$\% \text{ extension} = \frac{(\text{final} - \text{initial})}{\text{final}} \times 100$$

$$\% \text{ extension} = \frac{(17400\text{ft} - 16450\text{ft})}{16450\text{ft}} \times 100 = 5.78\%$$

3.4 Detailed Stratigraphy

The composition and lithology of the Abiquiu is difficult to identify and was originally classified as “The Abiquiu Tuff” (Smith, 1938). Upon further observation it becomes clear that there are terrigenous depositional facies defining the large-scale stratigraphic texture of the outcrops.

Despite much of the Abiquiu formation seemingly subhorizontal and most-commonly associated with unconfined sheetflow deposits, there are also broad channels throughout exhibiting trough-cross stratification as well as other channels dominated by poorly sorted material ranging from fine-sand to subrounded boulder-size clasts. The grainsize of the Abiquiu formation is mostly fine-to-medium sand and composed of predominantly volcanic quartz, lithic fragments, and volcanic ash. The Abiquiu formation is a volcarenite sandstone and in many places considered an unconfined hyperconcentrated sheet flow deposit. There are three to four intervals of the Abiquiu Formation that are defined by lithologic composition and sedimentary facies. There are many channels within the Abiquiu Formation that transport larger material, suggesting periods of higher energy within the unconfined depositional environment. Previous studies and this study suggest that the volcanoclastic material is sourced from the Oligo-Miocene San Juan and Latir volcanic fields to the north-east and north-west in southern Colorado and Northern New Mexico (Smith, 1995).

3.4.1 Measured Stratigraphic Sections

Several measured stratigraphic sections in the Plaza Blanca area show variation on sedimentary facies across the fault system. The primary purpose of measuring the stratigraphic sections is to both estimate the thickness of the faulted Abiquiu and to evaluate the magnitude of throw across the fault system based on stratigraphic correlation of the measured sections.

Sections A and B from figure 3.4 are located in the footwall of the Plaza Blanca Fault. The two sections are measured from different sides of the Plaza Blanca Canyon and show clear correlation

with a definite marker bed at 22.45 m in each section as well a similar facies change at approximately 45m. There is a change in facies from massive fine-to-medium grained sandstone interbedded with clay-to-silt size beds to a more channel dominated facies showing coarse-grained trough-cross bedding amalgamated with poorly sorted conglomeratic beds with cobble and rare boulder-size clasts of metamorphic and volcanic origin. The change in facies is interpreted as the shift from interval II pumaceous and tuffaceous lithic clasts in a sheet flow dominated environment to Interval III dominated by channelized pulses of sedimentary material. Compared to measured section D located in the hanging wall of the Plaza Blanca Fault system sections A and B are quite different. Section D exhibits the facies expected with Interval III, coarse grained material in a channel dominated sedimentary facies. Section D does not, however, depict the stratigraphic contact between interval II and interval III as section A and B do. This suggests a minimum throw estimate to be ~40m across the fault system (Figure 5.1).

Stratigraphic sections measured at various key locations across the Plaza Blanca canyon include the foot wall, accommodation zone, and hanging wall of the Plaza Blanca fault zone. A Jacob staff was used to measure the sections. Observations were made to interpret sedimentary facies and determine grainsize, and compositional changes in the Abiquiu Formation.

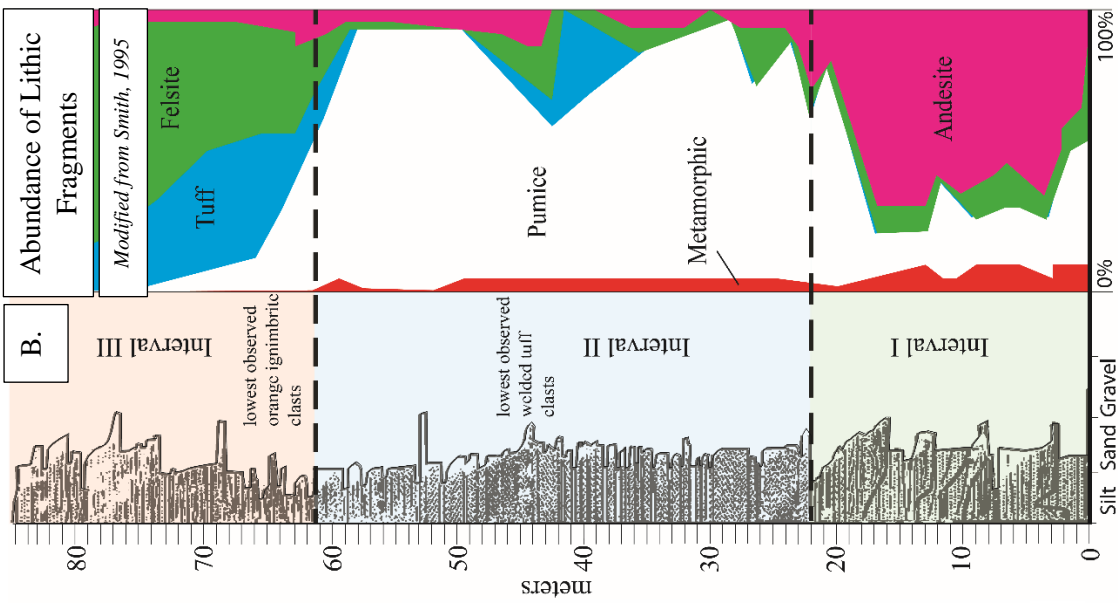
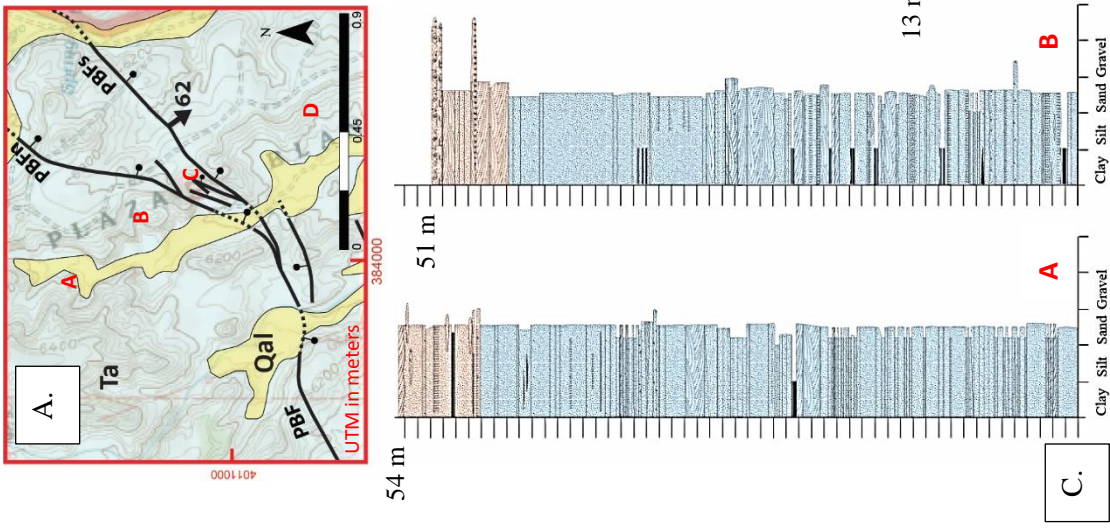


Figure 3.4: Identifying the subtle intervals of the Abiquiu Formation is critical to both understanding the Abiquiu Formation and to determine the magnitude of throw across the Plaza Blanca fault splay. The red letters correspond to the map (A.). A. is a regional map showing measured section locations. B. is a stratigraphic section compiled by Smith, 1995 showing abundance of lithic fragments and the intervals of the Abiquiu. C. interpreted measured sections. Orange is interval III blue is interval II. Scale of B. and C. are the same.



4. METHODS

4.1 Regional

Two methods are employed to identify fracture populations. The first method is a way to collect a vast amount of fracture data through a modified circular-window method applied directly to the rock surface in the field. The other method is to utilize Gigapan imagery to take a high-resolution panoramic views with the purpose of detailed fracture annotation and later apply the circular window method to the virtual outcrop. By combining these two techniques with detailed geologic mapping it is possible to quantify large fracture patterns and populations associated with Rio Grande rift extension in three dimensions.

Geology

- Fracture Windows
- Structural Interpretation
- Thin Section

Cartography

- Field Mapping
- ArcMap, Move, Adobe Illustrator

Fracture Collection and Visualization

GIS

- Annotation
- Field Move Clino
- ArcMap

Visualization

- Gigapan

Figure 4.1: These are the four pillars of the project. The combined aspects allow for a comprehensive quantitative fracture study that employs some novel methods.

4.2 Fracture Circles

There are two major sampling methods in outcrop-based fracture characterization: scan line, and areal sampling. The one-dimensional scan line method is subject to biases from orientation and length of the line, as well as fracture pattern heterogeneity (Rohrbaugh et al., 2002). In the areal sampling method, two shapes of sampling window exist: a rectangle, and a circle. I choose the circular window in order to avoid potential orientation bias posed by the rectangular window method.

The diameter of the circular window is two meters and is physically drawn on the ground surface of the desired location. The circle is drawn with an apparatus constructed of plastic (PVC) pipe that forms a right angle and resembles a large compass. On the long arm of the compass one meter is measured and a weight is attached to a length of rope to act as a guide for drawing the circle. This is a two person job, with one person holding and rotating the compass while the other follows the weighted guide and draws the circle. The final product may not look like a perfect circle from an oblique viewing angle due to the irregular ground surface but it does appear circular from the birds eye view. Once an adequate circle has been drawn, the fractures are then measured. The measurements collected are attitudes (strike and dip), fracture length, aperture of the fracture, fracture fill, intersection of the fracture with the drawn circle (N), elementary connective facets (I, X, Y). The elementary connective facets include fracture ends (I), abutting fractures (Y) and Crossing fractures (X) (Sanderson and Nixon, 2015). The use of cellular phone technology circa 2015 is used to collect and record large scale data sets. Field Move Clino Pro was used with a Samsung Galaxy S5 for the attitude measurements. Regular recalibration is necessary for the application to function consistently. Regular monitoring of the location properties is necessary to maintain accurate GPS location (typically within 3M radius). Using the Google Sheets spreadsheet technology on a separate device in the field was also employed for

quick data cataloguing and easy sharing once internet became available. Solar-panel charging allowed for the handheld devices to maintain battery life during long bouts of data collection. The GoalZero Nomad 7 solar panels work best in full sun.

Over 20 circles were sampled at key locations throughout the Plaza Blanca Fault Splay. This includes data from the fault core, splay zone and splay point (or branch line depending on dimension). Fractures of lengths ranging from 10 m to mm scale are measured.

This information is critical to understanding the fundamental relationships of the damage zone as it relates to the normal fault splay in the Plaza Blanca Region. There are many scaling relationships that are observed as well as fracture frequency relationships with proximity to the fault core.

Over 1200 fracture measurements were collected at a variety of scales ranging across 4 orders of magnitude. This tactile collection of information is a modified method of existing window methods that have previously been used to sample fracture populations involved in fault damage zones. The novel method employed for this study is the circular window method. A combination of the scan line method and circular window method is ideal however the complex topographic terrain of the Plaza Blanca Fault outcrop location does not lend to such a systematic sampling procedure. Thus the circular window method is applied at opportune locations both distally, proximally, on, and in the splay zone of the Plaza Blanca fault.

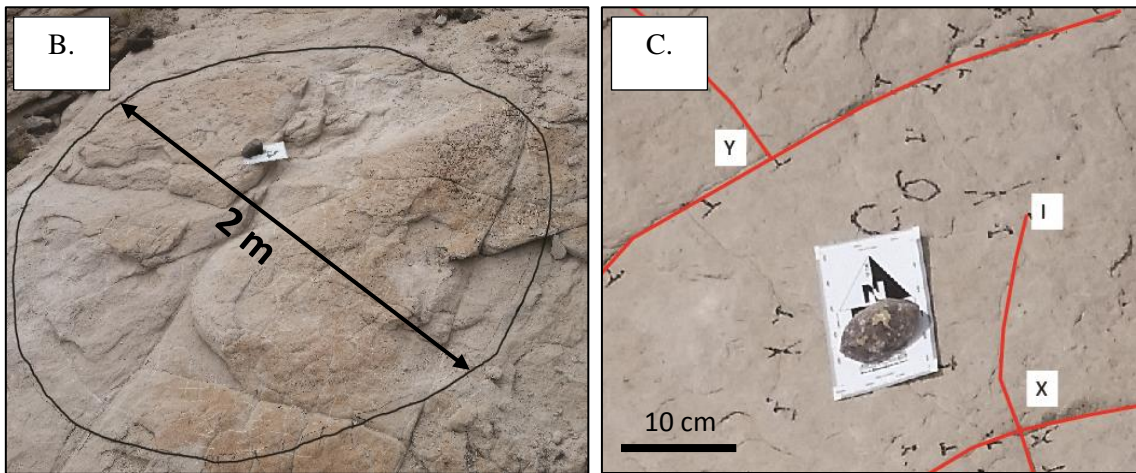
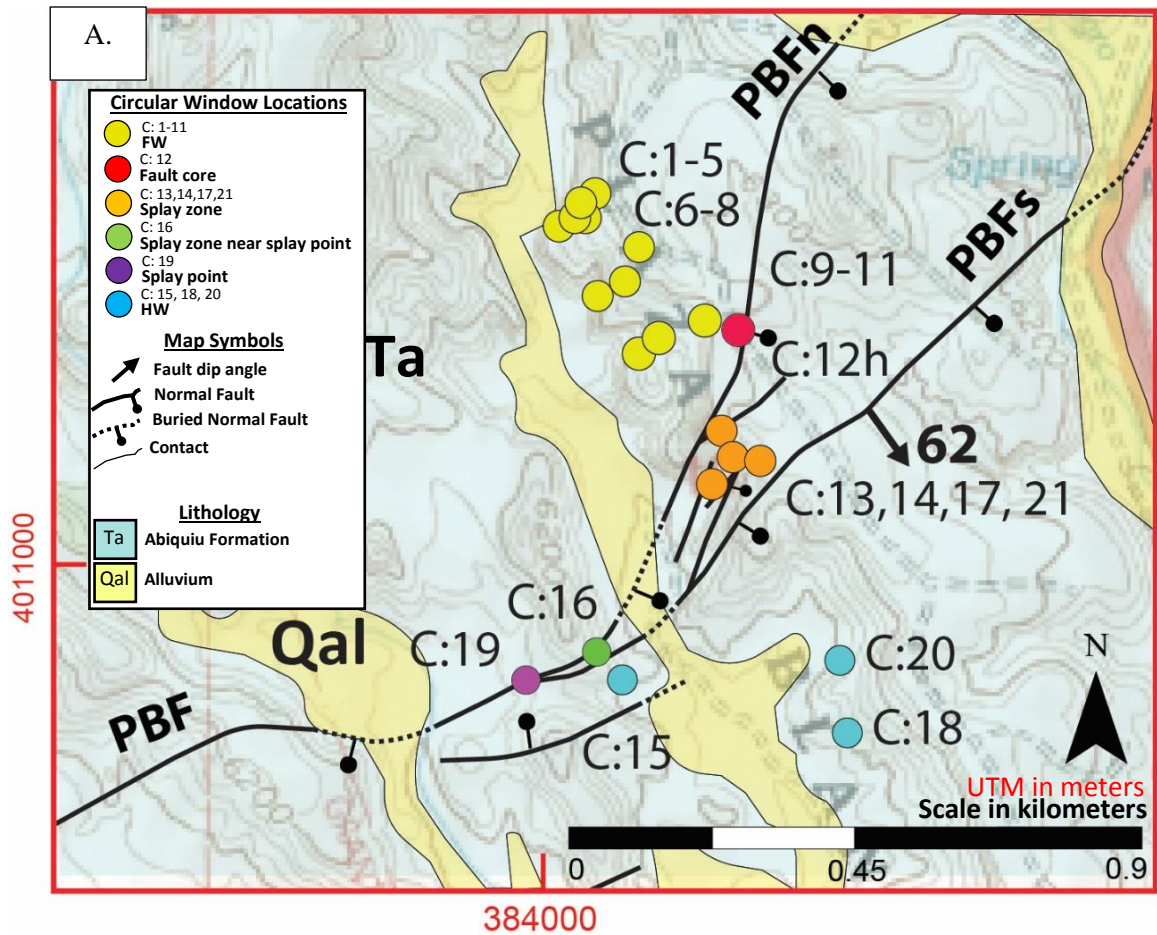


Figure 4.2: A. The location of the fracture circles (Colored circles) with respect to the Plaza Blanca Fault (PBF) splay showing the Plaza Blanca Fault north (PBFn) splay and the Plaza Blanca Fault south (PBFs) splay. B. The 2 meter diameter circular window outlined on the ~1 meter thick bed plane. C. Fracture attitudes (strike/dip), length, and connective facets are measured within each circle.

4.3 Gigapan Imagery

The use of high-resolution imagery is applied to further characterize fracture networks. The technology used is a Gigapan Epic Pro robotic mount and a Nikon D3100 digital camera with Nikon Af-S DX VR Zoom-Nikkor 55-200mm f4-4.5G IF-ED lens and sun shade on a Manfrotto 55XPROB tripod with a Manfrotto 804RC2 pan and tilt head with bullseye levels.

Once assembled and leveled at the location of interest the Gigapan needs to be calibrated. First the field of view is set by identifying the horizon with the top and bottom of the camera view. Next the corners of the total panoramic are set. The camera must be in full manual mode and the setting must be appropriately set for adequate light exposure. The robot then takes pictures on a grid which are a mosaic of zoomed in 22 megapixel images stitched together using the provided software to create one large panoramic image of gigapixel resolution. This allows for detailed fracture annotation at both wide and narrow scales. Depending on the proximity to the outcrop, fractures of up to centimeter scale may be identified. The digitized fracture network provides a fracture map of the outcrop. This two dimensional representation of the fracture network allows for fracture frequency calculations as well as the application of the elementary connectivity properties (I, X, Y). This map combined with the grouped surface measurements provides insight to the three dimensionality of the damage zone along the Plaza Blanca fault.

The locations for which Gigapan images were taken include a wide view of the Plaza Blanca fault splay facing the East, facing toward the splay point to the west, and various background outcrops on either side of the fault splay. For the purpose of this study only one Gigapan image will be specifically studied. This is referred to at the Plaza Blanca east splay wide. The images were collected at approximate 2 pm and it took 11 minutes to collect.

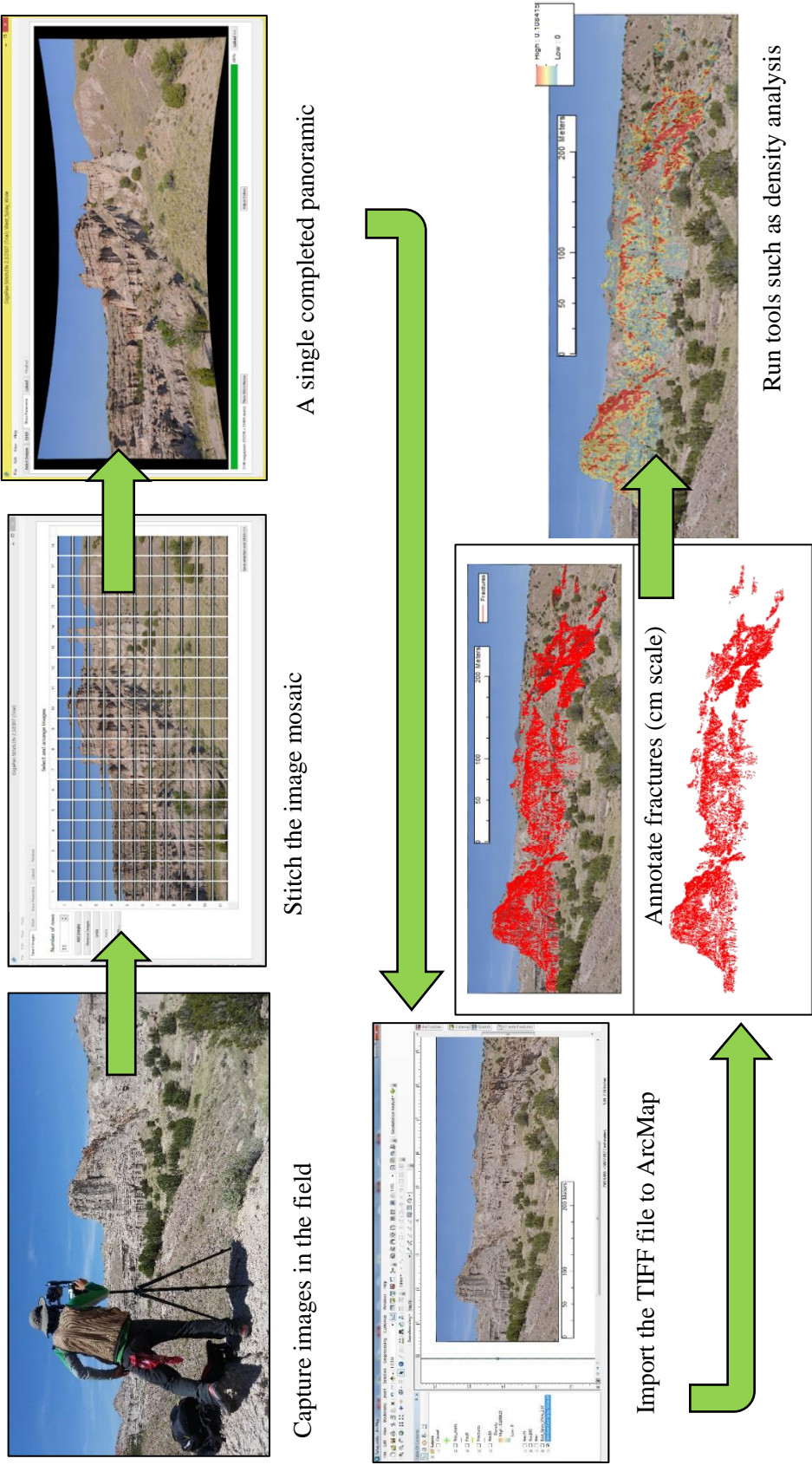
Interpretation of the fractures is conducted in ArcMap software. This may provide the potential to create a more robust three dimensional representation of the damage zone in the Plaza Blanca

region. The difficulty with using a two-dimensional image for constructing a three-dimensional model is the same difficulty as 3D seismic. Without a density of scan lines the resolution may not be adequate in some areas lacking visual outcrop. On the other hand, the detail of small-scale fracture annotation surpasses low-resolution seismic reflection images and rivals high-density LIDAR scans (Zahm and Hennings, 2009). In fact a LIDAR scan may be coupled with the Gigapan imagery in a future study.

The window method used for the fracture measurements and analysis on the ground surface is applied to the Gigapan outcrop images. A combination of scanline and circular window methods is applied to give a broad representation of the fractured damage zone across two connected faults. Structural geometric relationships such as Riedel shear and conjugate fracture geometries are identified in the detailed outcrop fracture map.

The outcrop-scale Gigapan also allows for inspection of fractures that are inaccessible due to high topographic relief and rugged terrain. It allows for more-detailed sampling of the fracture network at a larger scale through the remote sensing style of geology. There is also the ability to correlate bedding planes to determine both broad scale sedimentary facies as well as displacement variations across the fault splay zone. The breadth of the damage zone is important to addressing the overall relationship to throw and the extent of damage associated with synrift faulting in the Abiquiu formation.

The gigapixel imagery may also prove useful in determining the potential for fluid flow through the fracture network and compartmentalization of any such fluid due to fault or fracture sealing. The sealed fractures may be identified in hand sample or even in imagery and noted on the image which fracture is sealed or which is open.



Capture images in the field

Stitch the image mosaic

A single completed panoramic

Import the TIFF file to ArcMap

Annotate fractures (cm scale)

Run tools such as density analysis

Figure 4.3: A work flow description of Gigapan process. From capturing the images in the field to running a line density interpolation tool in ArcMap.

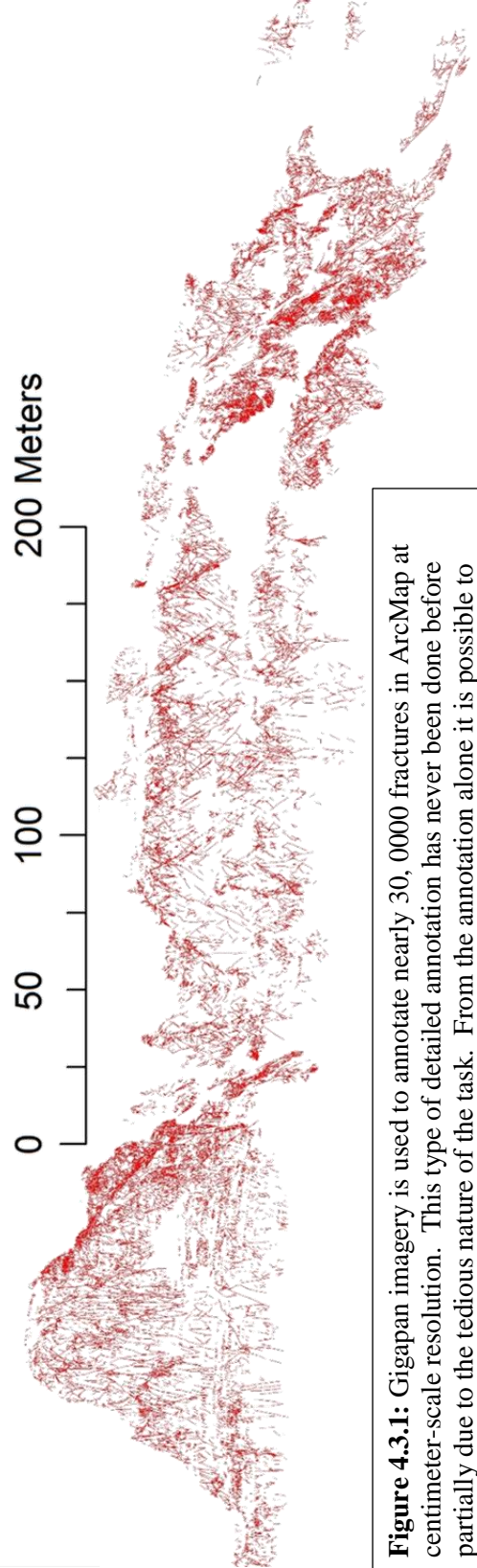
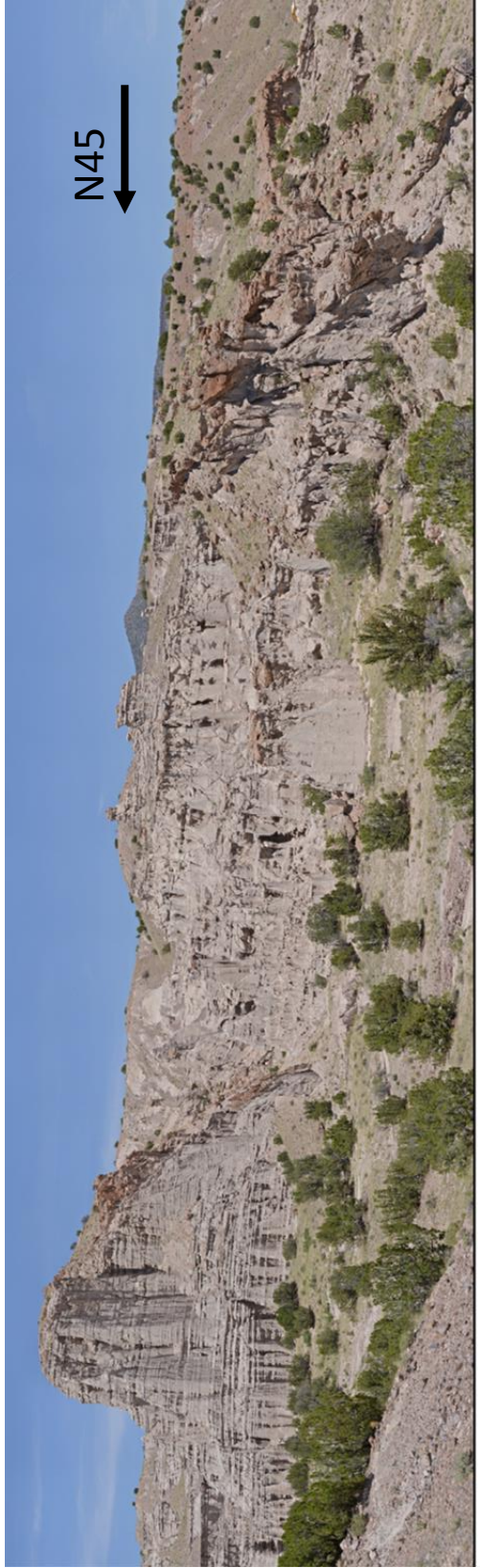


Figure 4.3.1: Gigapan imagery is used to annotate nearly 30, 000 fractures in ArcMap at centimeter-scale resolution. This type of detailed annotation has never been done before partially due to the tedious nature of the task. From the annotation alone it is possible to identify faults and zones of high fracture density.

4.4 Thin Sections

Samples were collected across the Plaza Blanca Fault (PBF) splay zone with the intention of producing thin sections (Figure 5.2). The reasoning is to assess the fracture-fluid flow interactions within the Abiquiu Formation at microscopic scale and then to compare that to fault core samples and splay zone samples. Identifying microstructures can assist in determining the relationship between fracture density and porosity. Microfractures can trap gasses, fluids, and cements as well as provide further insight to the stress near a fault core (Anders et al., 2014). The thin sections were viewed and captured using a Nikon Eclipse LV100POL microscope mounted with a Nikon DS-FI1 camera connected to a desktop PC.

The distal background sample serves as a baseline for assessing deformation associated with regional extension. The background sample (Figure 5.2.1 A.) is submature with angular to subangular moderately sorted grains ranging in size from 500 μm to $\sim 100 \mu\text{m}$ but with an average grainsize of $\sim 200 \mu\text{m}$. It is composed of minerals such as predominately volcanic quartz with minor plagioclase, microcline, biotite, chlorite, among other accessory minerals such as a rare zircon. Lithic fragments such as quartzite, granite, foliated metamorphic, vitric-pumice, and devitrified welded tuff are also present (see also Smith, 1995). These grains have been reworked during transportation and cemented by an ashy matrix. There seems to be a calcite rind around many of the grains indicating the presence of calcite cement. The grainsize and angularity is relatively homogenous throughout. There are no large veins and little to no evidence of microfractures associated with faulting. The splay zone sample (Figure 5.2.1 B.) has a similar composition of the background sample with an abundance of volcanic quartz but has an average grainsize of $100 \mu\text{m}$. It is well to moderately sorted with subangular to subrounded grains. There is a large devitrified welded tuff grain in the upper right corner that is $\sim 800 \mu\text{m}$ along the long

axis. It is noted that there appears to be calcite cement (for thin section images see Figure 5.2.1). Microfractures tend to accumulate in large grains.

5. RESULTS

Structural analysis across the Plaza Blanca fault zone reveals that it is a relatively large normal fault splay which can be imaged by seismic reflection methods. Analyzing the fracture network properties in this splay zone should provide useful information for understanding the underground fracture networks.

5.1 Throw

The throw across the Plaza Blanca faults is approximately 45 meters. This estimation is determined from correlating measured sections collected in the field. Previous studies show a correlation between damage zone width and throw (O’Keeffe, 2014). It is important to have a proper estimate for throw in order to make assumptions about strain when looking at a fracture network. The Abiquiu formation has a subtle and often ambiguous stratigraphy. It does have some diagnostic properties such as sedimentary facies changes and composition of lithic fragments. The Abiquiu formation has been previously classified into intervals. Using the intervals provided by Smith, 1995 the collected measured sections in the foot wall show a distinct contact in facies change. This is interpreted as the contact between interval 2 and interval 3. The absence of interval 2 in the hanging wall indicates a minimum throw equal to that of the exposed interval 2 in the footwall. It is unclear how the total throw is partitioned across the fault splay. Stratigraphic correlation in the splay zone is inconclusive and therefore cannot be quantified.

A cross section of the Abiquiu formation (A-A’) crosses the Plaza Blanca faults as well as faults in the southeast. The total percent extension in the Plaza Blanca region is ~5.78% with 290 meters of extension across the fault zone. In the cross section I interpret the PBFs to accommodate the majority of the fault displacement based on its longer regional length (Figure 3.2). This total E-W horizontal extension of nearly 300 meters than the total throw across the region must exceed 300 m. If this is the case the total throw across the Plaza Blanca region exceeds the throw of the Cañones Fault.

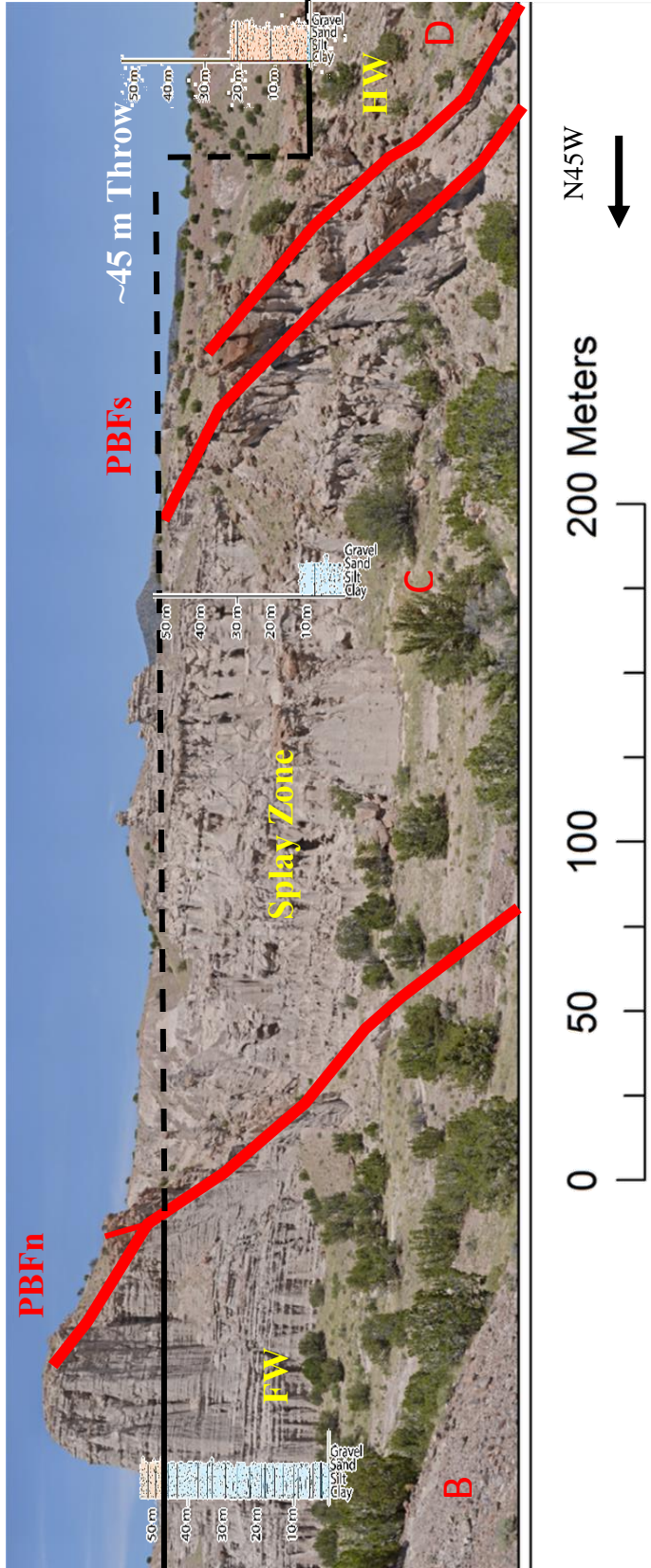


Figure 5.1: Using measured stratigraphic sections to estimate throw across the Plaza Blanca Fault. Based on Measured Sections B, C, and D it is possible to estimate a throw of ~45 m across the entire fault splay. For a more detailed look at the stratigraphic sections see Figure 3.4.

5.2 Microstructures

The background sample is used as a baseline for describing the thin sections. A detailed description of the method is in section 4.4. The fundamental difference between the background and the splay zone is the texture. The grain size is smaller, the grains are more rounded, and well to moderate sorting suggests the splay zone is more mature than the background. This is most likely due to different location in stratigraphy but may also be due to grain size reduction during deformation, although no microstructures or veins can support this from a lone thin section.

The most striking observation when looking at Figure 5.2.1 A and B compared to the fault core samples is the clear evidence of deformation. Cataclasis, grain size reduction, millimeter sized veins, microstructures depicting minute offset and syntaxial quartz growths are examples of some microstructural deformation at the fault cores. The samples were collected from the north west and south east sides of exposed fault cores both at the PBF north and PBF south. Each thin section depicts different line of evidence suggesting fluid interaction with faulting.

Figure 5.2.1 C. is from the PBF north fault core on the northwest or foot wall side of the fault. Mode I style fractures have syntaxial quartz growths and zones of catalasite with calcite and clay cement. The predominant fault surface is 1 mm wide and has shear fractures in conjugate or maybe R' geometries.

Figure 5.2.1 D. is from the PBF north fault core on the southeast or hanging wall side of the fault. This view depicts an open vein 500 μm wide, for which a mix of clay and siliceous cement has intruded. Out of the field of view are several other fine grained zones for which fluid passed through.

Figure 5.2.1 E. is from the PBF south fault core on the northwest or foot wall side of the fault. A vein ~200 μm wide filled with chalcedony crosses the field of view. Offsets of ~10 μm along shear microfractures cross cut the vein.

Figure 5.2.1 F. is from the PBF south fault core on the northwest or hanging wall side of the fault. Zones of grainsize reduction and microfractured grains are seen here. A clay rich cements the smaller grains in a similar orientation to the vein from PBFn SE.

It appears as if there is more shear fractures and siliceous cement in the footwall side of the fault. The hanging wall side of the fault shows more clay rich cements in open veins. Both sides of the fault show evidence of microstructures interacting with fluid that create cements of various compositions. (With the help of Scholle et al., 2014)

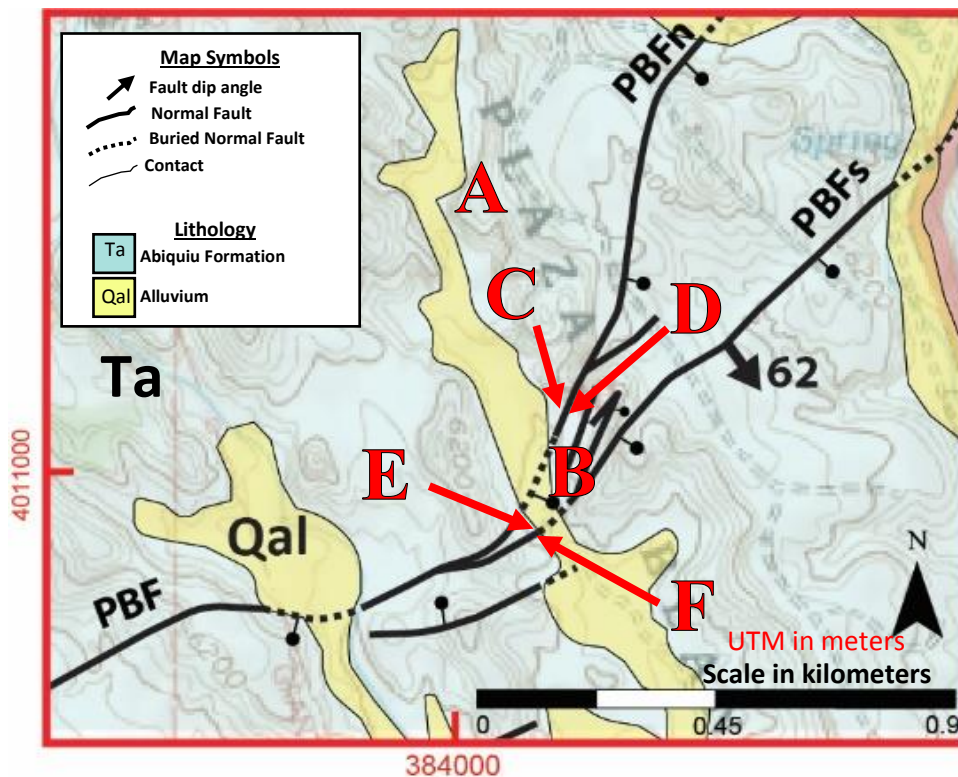


Figure 5.2: This map of the Plaza Blanca Fault (PBF) splay depicts the north splay (PBFn) and the south splay (PBFs) with location of the sample collection for thin section analysis. The letters correspond to

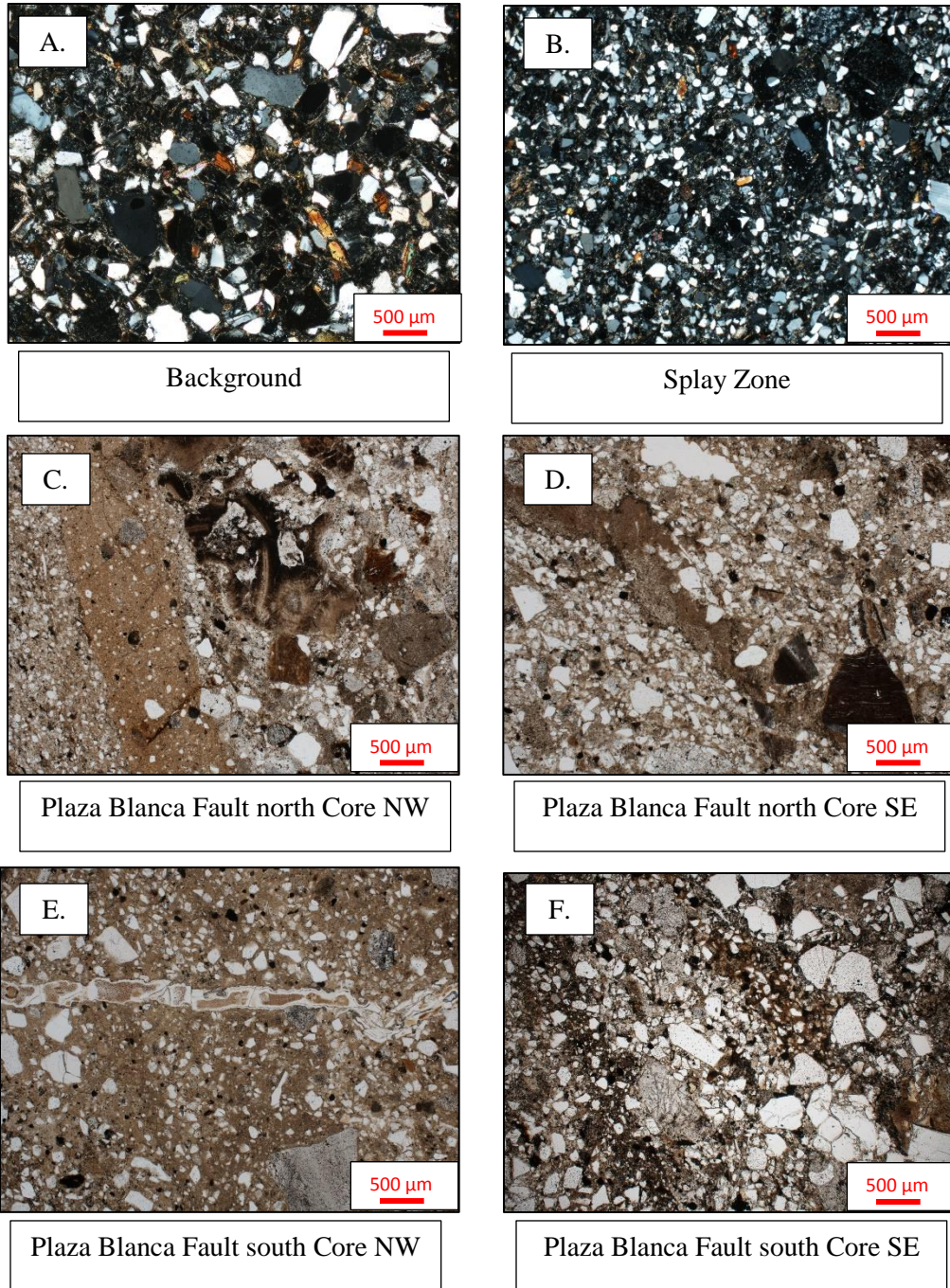


Figure 5.2.1: Thin sections are under 2.5X magnification. A. and B. are from the background of the damage zone and in the splay zone (see Figure 5.2). They are in cross polar light to depict grain size, sorting, and angularity better. C.-F. are from the Plaza Blanca Fault cores (Figure 5.2) and are in plane polar light to better depict the microstructures.

5.3 Width of the Plaza Blanca Fault Damage Zone

Damage zones surrounding a single fault become broader as faults interconnect (Faulkner et al., 2010). As throw increases the damage zone also widens. The broader the interconnected fault zone the broader the associated damage zone. At this fault splay the damage zone becomes more complicated as two major faults interact. The predicted width of the damage zone in this region based on the throw of the fault should be ~ 45 m. Of course this depends on how fracture density defines the damage zone.

Detailed quantitative fracture analysis using a 2 m diameter-window method on bed surfaces at various locations across the fault zone shows fracture-density variations. Fracture density at ~ 200 m from the fault core is < 20 fractures per circle and defined as background damage. Fracture density is 400 fractures per circle on the fault core as well as a heightened fracture frequency in the accommodation zone between two connected faults with 150-200 fractures per circle. There are 600 fractures at the branch line of the two faults showing a 50% increase in fractures where two faults intersect. Fracture scales and geometries vary with respect to proximity to the fault core.

In Figure 5.3.1 yellow zone 2 begins to move to a slightly denser fracture zone. If we call this the edge of the PBFn foot wall damage zone then the width is ~ 20 m. This zone increases to the southeast as more faulting occurs and the faults begin to connect thus widening and blurring the boundary of the damage zone for the single fault. Previous studies show a positive correlation between magnitude of damage zone width and magnitude of throw (Figure 5.3). The damage zone width of PBFn is plotted above as a yellow star by doubling the footwall width and halving the total splay throw to ~ 20 m. By measuring the total width of the damage zone associated with the splay then the overall throw of ~ 45 m corresponds to a total width of ~ 60 m which is still reasonably correlative to Figure 5.3. As faults connect damage zone do not uniformly widen.

This is best illustrated in Figure 5.3.1. Density based on the tactile fracture window collection compared to locations of fracture circle windows across the splay zone show clear density spikes. The colored circles on the key map match the colored locations on the graph. The yellow zone marks the fracture density in the foot wall of the PBF. The red zone is a density spike at the fault core of PBFn. The orange circle is the zone within the fault splay as is the green yet the green zone is more proximal to the splay point. The Purple zone is another density spike at the splay point. The blue zone represents fracture density in the hanging wall of the Plaza Blanca fault splay.

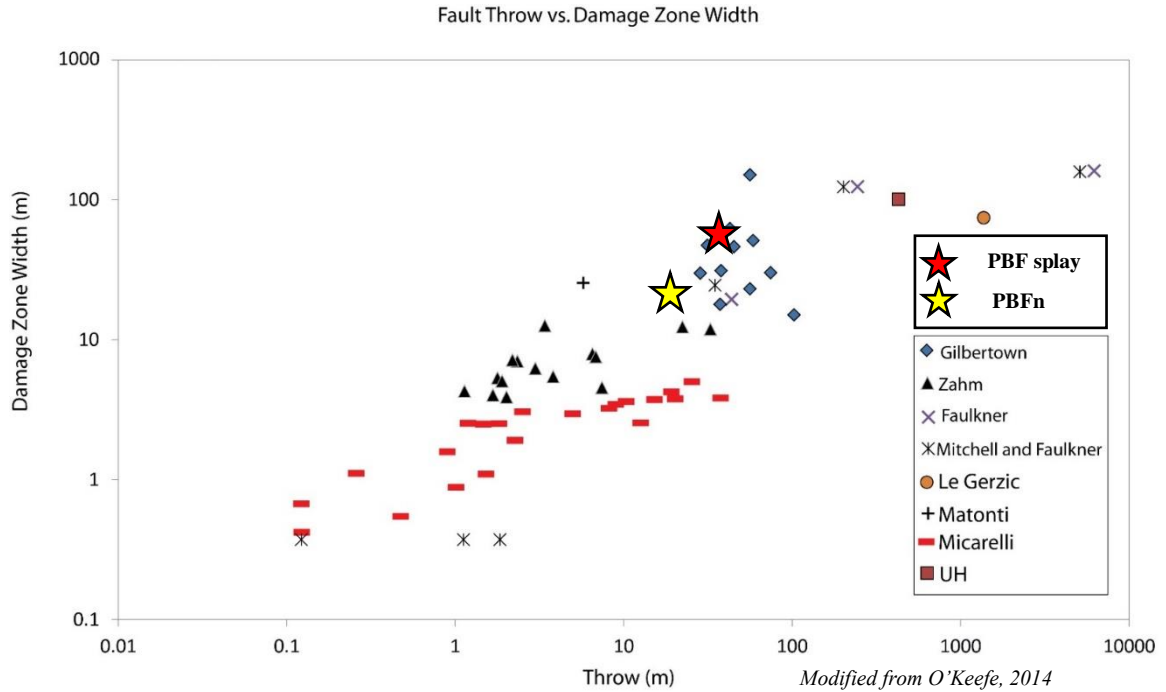


Figure 5.3: Previous studies show a positive correlation between magnitude of damage zone width and magnitude of throw. In Figure 5.3.1 below yellow zone 2 seems to begin a move away from background level of fracture density to a slightly denser zone. If we call this the edge of the damage zone then the width of the damage zone is approximately 25 meters in the footwall. The damage zone width of the Plaza Blanca Fault north (PBFn from key map in Figure 5.3.1) is plotted above as a yellow star.

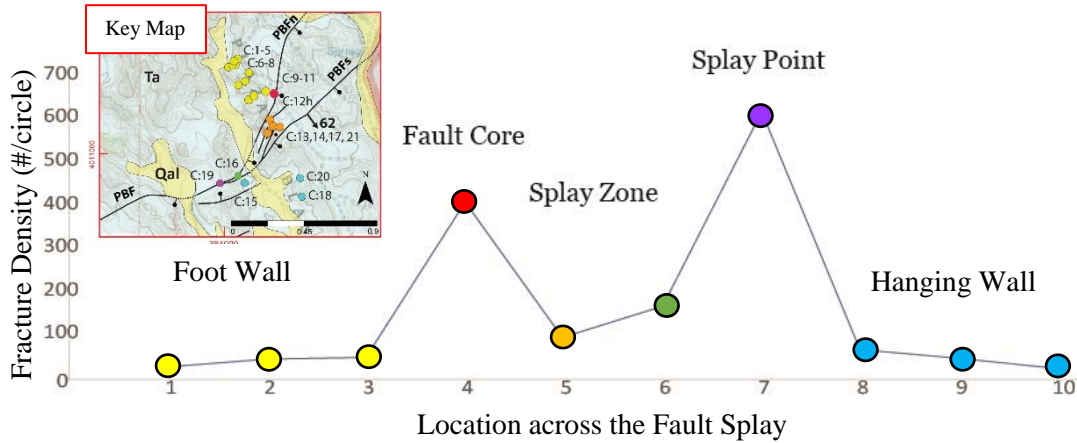


Figure 5.3.1: Fracture density based on the tactile fracture window collection vs. locations of fracture circle windows across the splay zone. The colored circles on the key map match the colored locations on the graph. The yellow zone marks the fracture density in the foot wall of the Plaza Blanca Fault. The red zone is density at the fault core. The orange circle is the zone within the fault splay as is the green yet the green zone is more proximal to the splay point. The Purple zone is density at the splay point. The blue zone represents fracture density in the hanging wall of the Plaza Blanca fault splay.

5.4 Fracture Characterization

Fracture mechanisms, geometry, density, and connectivity are key components to understanding and characterizing fracture networks. It is important to think of fracture networks as dynamic features that change through time, albeit geologic time, to accommodate strain. During the formation and maturation of a fault, the timing of damage zone fractures is important to understanding strain partitioning.

5.4.1 Fracture Mechanisms

The Plaza Blanca Fault (PBF) core is the primary displacement zone (PDZ). The fracture damage zone that surrounds the PBF may have a variety of fracture mechanisms typically associated with a PDZ. This may become further complicated with the concept of linked fault cores. Fractures have been known to enhance permeability provided they remain open. Fault cores are shear zones that significantly reduce permeability. This is primarily due to reduction of grain size during faulting, cataclasis, and incorporated clays to the fault core. A poorly sorted fault core creates more of a seal than a pathway. Figure 5.4.1 C. depicts a widening damage zone as faults overlap, bend, link, and propagate (Peacock et al., 2002). Studying interacting faults are important for understanding fracture damage zone development. The variety of fracture modes relate to the principle stresses that are applied to the unreformed protolith. This includes a variety of shear fracture geometries as well as open fractures. How these types of fractures interact to accommodate strain is applicable to understanding the potential for permeability enhancement in a fracture network (Shipton and Cowie, 2003). Figure 5.4.1 A. shows the various modes of fracture style. Mode I style fractures are tension fractures that open in the direction of minimum principle stress. Mode II and Mode III fractures are shear fractures and may be represented by a PDZ oriented fracture, conjugate to the PDZ, and Riedel shear geometries. Mode III have a rotational component and may be seen at fault or fracture tips. Mode IV represents stylolites which are not observed in the Abiquiu Formation. A hybrid of modes I, II, and III show a potential for both shear and tension components of a fracture. This is most likely in the R style Riedel shear fracture. Figure 5.4.1 B. Shows a PDZ with accompanying conjugate and R, P, R' Riedel shear fractures. T is a mode I style tension fracture.

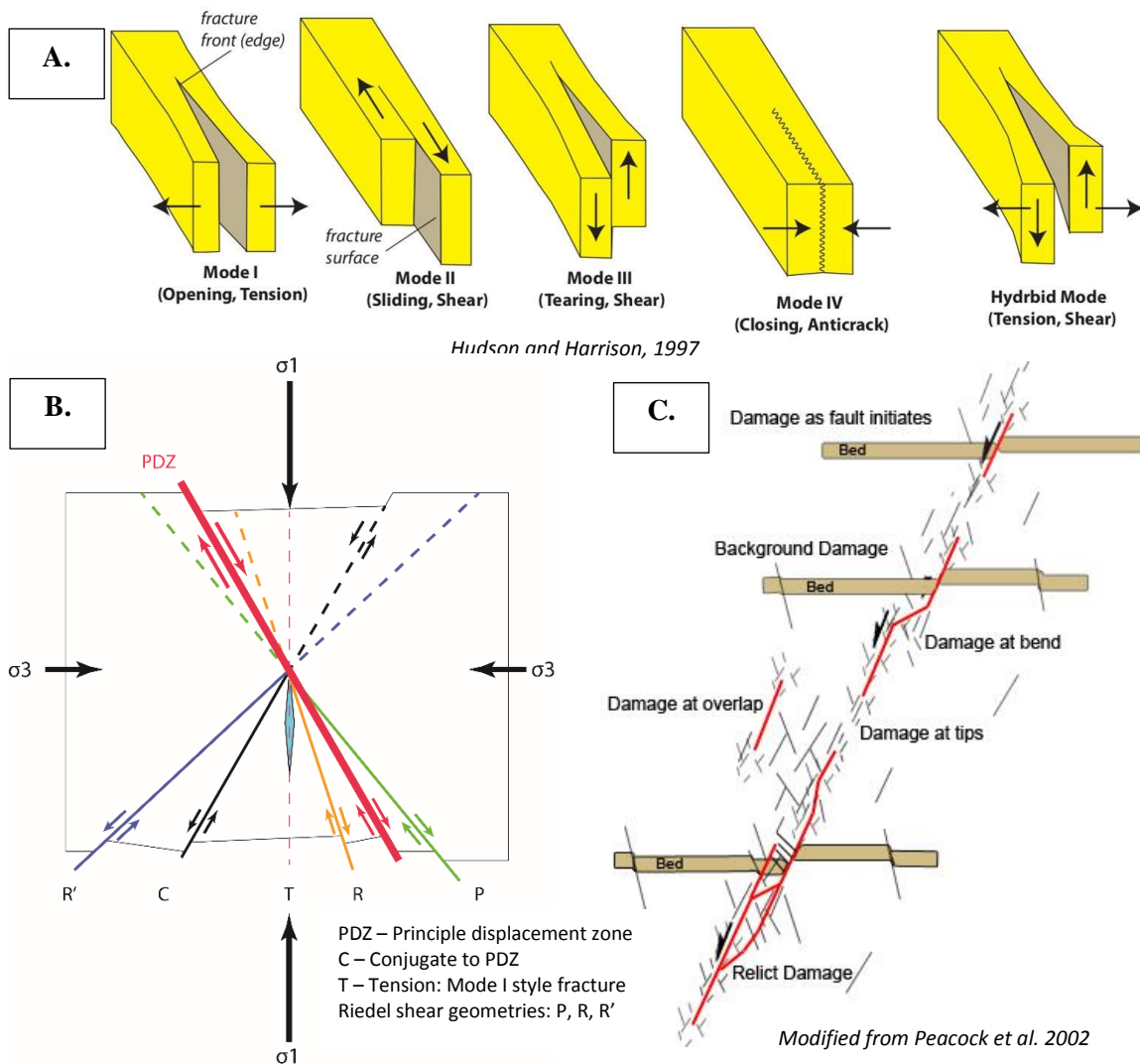


Figure 5.4.1: A. depicts the various modes of fracture style. B. Shows a principle displacement zone (PDZ) with accompanying conjugate and R, P, R' Riedel shear fractures. T is a mode I style tension fracture. C. Depicts a widening damage zone as faults overlap, bend, link, and propagate.

5.4.2 Fracture Geometry

Many poles to fracture planes from the circular window data are contoured to depict fracture orientations of all scales and locations. The result is a primary orientation of approximately N50E at all scales.

There are many geometric relationships in a multiple fault zone. These relationships are fundamental fabrics that produce complicated fracture networks produced in the damage zone resulting from fault development. Connected faults will broaden the damage zone and not only weaken the bedrock but complicate the permeability of an otherwise predictable porous lithology.

One key observation is the higher the fracture density, the smaller the fracture length per area. The more fractures per area the more irregular the fracture orientation. This is observed in stereonets of over 1200 fractures collected across the damage zone.

Riedel shear fracture geometries are typical near a principle displacement zone (PDZ) and include P, R, R' orientations (see Figure 5.4.1 B.). A principle displacement zone representing the fault core and kinematic slip surfaces with typical 60° dip has associated synthetic shear fractures and conjugate antithetic shear fractures. Tension fractures represent the mode 1 style and typical opening orientation perpendicular to the maximum principle stress (σ_1). These fractures and faults all become incorporated into a larger damage zone as faults link and the fracture damage zone becomes more complicated. Figure 5.4.2 shows 1200+ fractures collected from the tactile circular window method across the Plaza Blanca Fault splay. These fractures are plotted independently of location. The fractures are contoured poles to fracture planes of varying lengths independent of location in the splay. The scaling relationship of fractures by length shows a preferential orientation of approximately N45E in the longer fractures. The smaller the fracture the more chaotic the orientation becomes, possibly induced by the unloading process which bears no preferred orientations. All of the fractures show steep dips especially the smaller fractures.

Based on the geometric relationships from Figure 5.4.1 B, an assumption can be made that the steeper dip a fracture has the more prone it is to exhibit mode I style or a hybrid mode style of fracture. This insinuates that steeper fractures may be more prone to open and thus become conduits for flow and mechanisms for enhanced permeability.

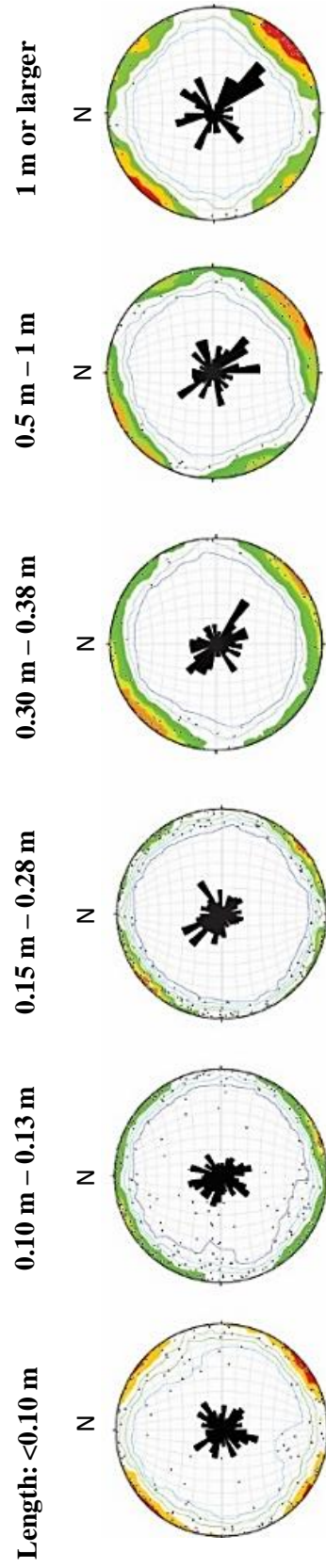


Figure 5.4.2: 1200+ contoured poles to fracture planes of varying lengths independent of location in the splay. This data is from tactile fracture collection in the circular fracture windows across the Plaza Blanca Fault splay. The scaling relationship of fractures by length shows a preferential orientation of approximately N45E in the longer fractures. The smaller the fracture the more chaotic the orientation becomes.

The annotated Gigapan image of the Plaza Blanca splay in Figure 5.4.2.1 depicts several fracture geometries. Some of the geometries can be predicted based on typical shear models. The examples of Riedel shear fractures near the fault core show how it is possible to identify fracture mechanisms from a two dimensional annotated fracture network. If the assumptions above about steeply dipping fractures being more prone to open style a detailed further characterization of fracture mechanisms based on geometry can be applied to a network with the potential for predicting transmissivity pathways in a damage zone. (Billi et al., 2003; Fossen, et al., 2005; Faulkner et al., 2010; Sanderson and Nixon, 2015; Watkins et al., 2015)

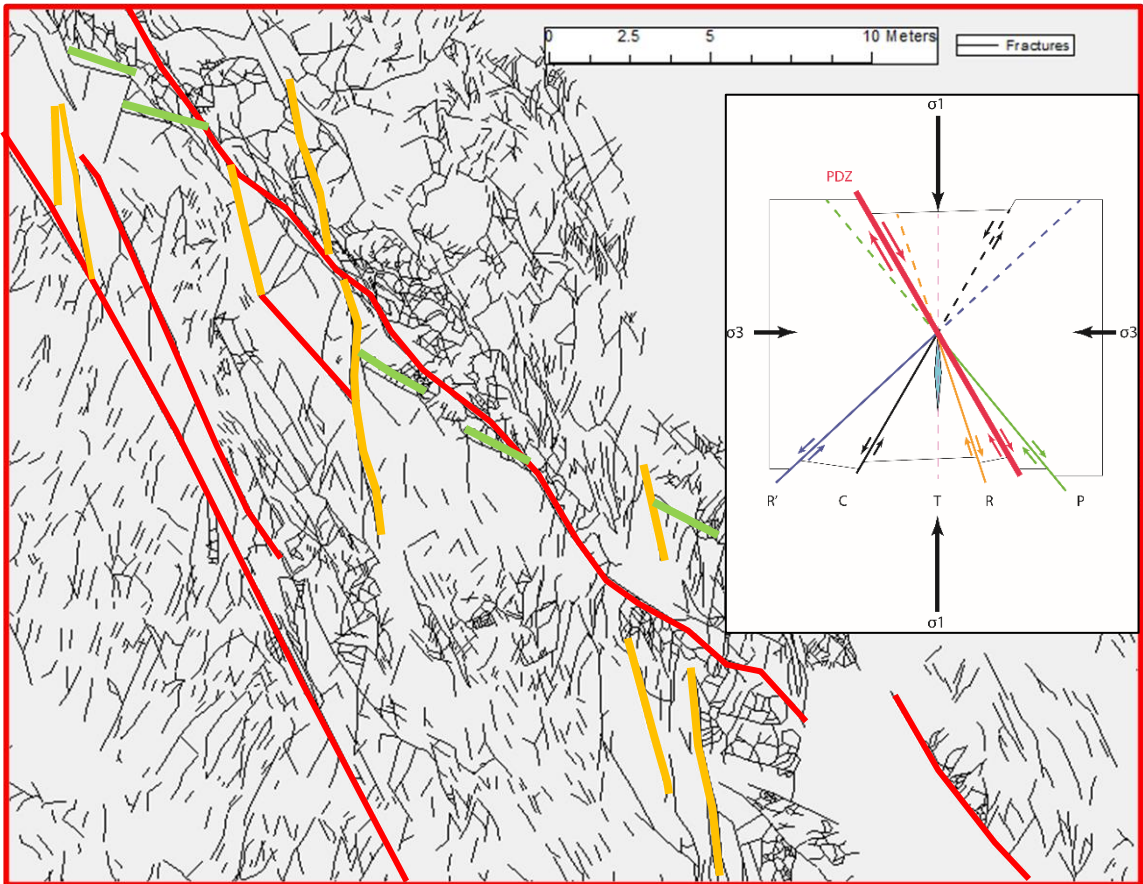


Figure 5.4.2.1: This is a section of selectively annotated fractures from the fault core and proximal regions. The view shows principle displacement zones (PDZ) in red and many conjugate fractures (C). Riedel R shears are in orange and P shears are in green. There may be tension (T), Mode I style fractures and other Riedel shears such as R'.

5.4.3 Fracture Density

Based on the tactile measurements from the circular windows it was determined that fracture density is lower in portions of the damage zone distal from the fault core and increases with proximity. In Figure 5.4.3 it is apparent that fracture density becomes approximately 8 times larger at the fault core. Fracture density in the accommodation zone, known as the “splay zone”, is greater than the damage formed by a single fault. Within the splay zone the fracture density increases with closer proximity to the “splay point” which is the surface expression of the branch line of two connected fault cores. The splay point has the highest fracture density, by increasing density by 50%.

The annotated Gigapan image is further characterized by running a line density tool in ArcMap. This produces a fracture density contour map that supports the quantitative observations from the circular window method. Area density= magnitude per unit area from a polyline feature that falls within a radius around each cell (frac10: Has cell size 10cm x 10cm with a nearest neighbor radius of 100 cm). This means that the High value of 0.108415 or 10.8 fractures per 1m² cell

Figure 5.4.3 A. Depicts the density contour outcrop without annotated fractures. The red regions represent the highest density of fractures which is mainly surrounding the immediate fault core. Figure 5.4.3 B. depicts a closer view of the Plaza Blanca Fault north splay with associated damage zone. There are several geometries of fractures depicted here. Figure 5.4.3 C. is a close up of the fault core. The fracture density is small, the fracture lengths are shorter, and the fracture orientation is becoming more erratic at small scales.

This density contour map goes a step further by highlighting the heterogeneity of the fracture damage zone. Certain regions of isolated high fracture density are readily observed distal to the fault core. Conversely linear regions of high fracture density reveal synthetic and antithetic faults showing continuous and homogenous high density zones. (Watkins et al., 2015)

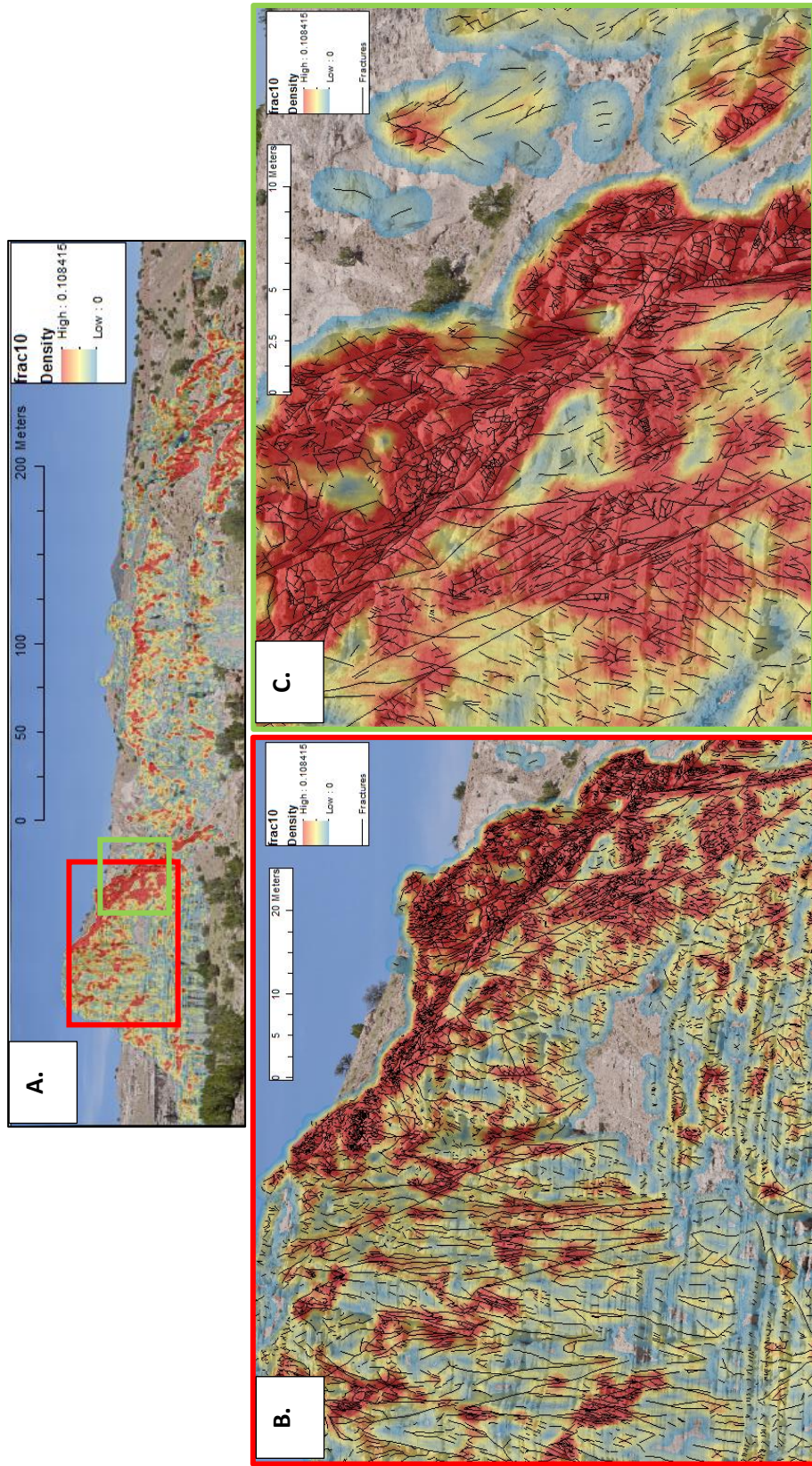


Figure 5.4.3: Gigapan contoured for fracture density. Area density= magnitude per unit area from a polyline feature that falls within a radius around each cell (frac10: Has cell size 10cm x 10cm with a nearest neighbor radius of 100 cm). This means that the High value of 0.108415 means there are 10.8 fractures per 1m² cell. A. Depicts the density contour outcrop without annotated fractures. The red regions represent the highest density of fractures which is mainly surrounding the immediate fault core. B. Depicts a closer view of the Plaza Blanca Fault north splay with associated damage zone. There are several geometries of fractures depicted here. C. Is a close up of the fault core. The fracture density is small, the fracture lengths are shorter, and the fracture orientation is more erratic at small scales.

5.4.4 Connectivity

Basic connectivity is a factor in understanding potential transmissivity through a network.

Identifying three fundamental connective facets: I for ends of fractures, Y for abutting fractures, and X for crossing fractures are part of the window analysis. These connective facets are then plotted on a ternary diagram where connectivity can be quantified. The higher fracture frequency the more connected the fractures are.

There is a trend between the fracture density and connectivity. Areas with higher fracture density have more connected fractures and potentially have a higher permeability. That does not necessarily enhance permeability though. Fluid flow in a fracture system is influenced by fracture orientations, heterogeneities, density, and connectivity (Watkins et al., 2015). During the tactile fracture collecting using the window method certain first order connective facets are noted along with the attitude and length measurements. Connective nodes I for the ends of fractures, Y for abutting fractures, and X for crossing fractures can be plotted on a ternary diagram (Sanderson and Nixon, 2015). In figure 5.4.4 relationships of location of fracture circle window with respect to its location on the ternary plot shows how connected per branch a fracture network is.

Connections per branch (C_B) is represented by *Equation 5.4.4*:

$$C_B = \frac{2(3Y + 4X)}{(I + 3Y + 4X)}$$

The higher the C_B value the more connected a network is. These values are represented on the ternary in Figure 5.4.4.B. on the right I-X side of the triangle. Specific fracture geometries are represented at different locations on the ternary suggesting possible ways fractures will connect with certain I, X, Y values (Sanderson and Nixon, 2015).

The yellow region of the footwall fractures lie in low to intermediate connective values ranging in C_B values of 1.2 to 1.8. The predicted geometries in these areas indicate longer more regularly

oriented fractures connected primarily by abutting relationships. This is also the case with the fractures in the hanging-wall damage zone. The fractures within the splay zone are overall more connected and sometimes extremely connected with C_B values between 1.9 and 1.95. The orange zone in the splay zone is more distal from the splay point and is less connected than the green zone which is within the splay zone but more proximal to the splay point. The orange zone has a different predicted geometry than the green zone. The green zone has more X (crossing) fractures than the predominantly Y (abutting) orange. As suspected the fault core of the Plaza Blanca Fault has an extremely high C_B value of >1.95 . The fracture geometry is chaotic and composed of many small fractures such as expected from the tactile study (see Figure 5.4.2). The fault splay point, represented by the purple zone, is also extremely connected with a C_B value >1.95 . The difference between the connectivity at the single fault core versus the connected fault cores at the splay point is that the splay point is more connected by X (crossing) fractures rather than dominated by abutting fracture geometries.

How a fault splay is formed is still an open question: whether two faults grow separately and join together, or a single fault bifurcates into two. The connectivity plot in this study lends support to the former model (Fossen et al., 2005).

A near linear correlation is observed between the sum of connective facets per circle vs the sum of total fractures per circle (Figure 6). Using this concept is fundamental to applying the concept of connectivity to a two dimensional high resolution Gigapan image of an outcrop. Detailed annotation of the Gigapan imagery reveals geometric and scaling relationships with proximity to various connected fault cores. In this study the combined methods for fracture characterization illustrates the importance of understanding fracture damage zones at several scales.

Structural style of the fracture, such as mode 1 opening fractures compared with Riedel simple shear mode 2 or 3 style fractures play a fundamental role in establishing preferred pathways. The

potential for reduced grain size or incorporated cataclasite in any shear zone is higher and more likely to reduce porosity and thus permeability. This may even reduce permeability if the grains become too unsorted. It has been noted that ideal porosity in a material is greater with better sorting and roundness. The ideal enhanced interstitial void then acts as a potential pore throat that, as a function of scale, increases the permeability of any solid material. Fractures may enhance permeability at any “mode I” style opening.

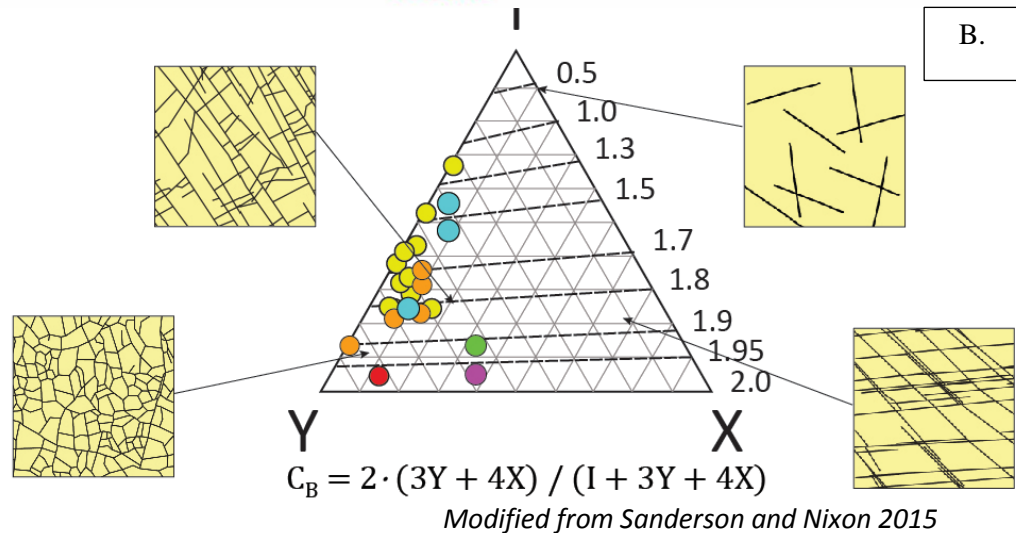
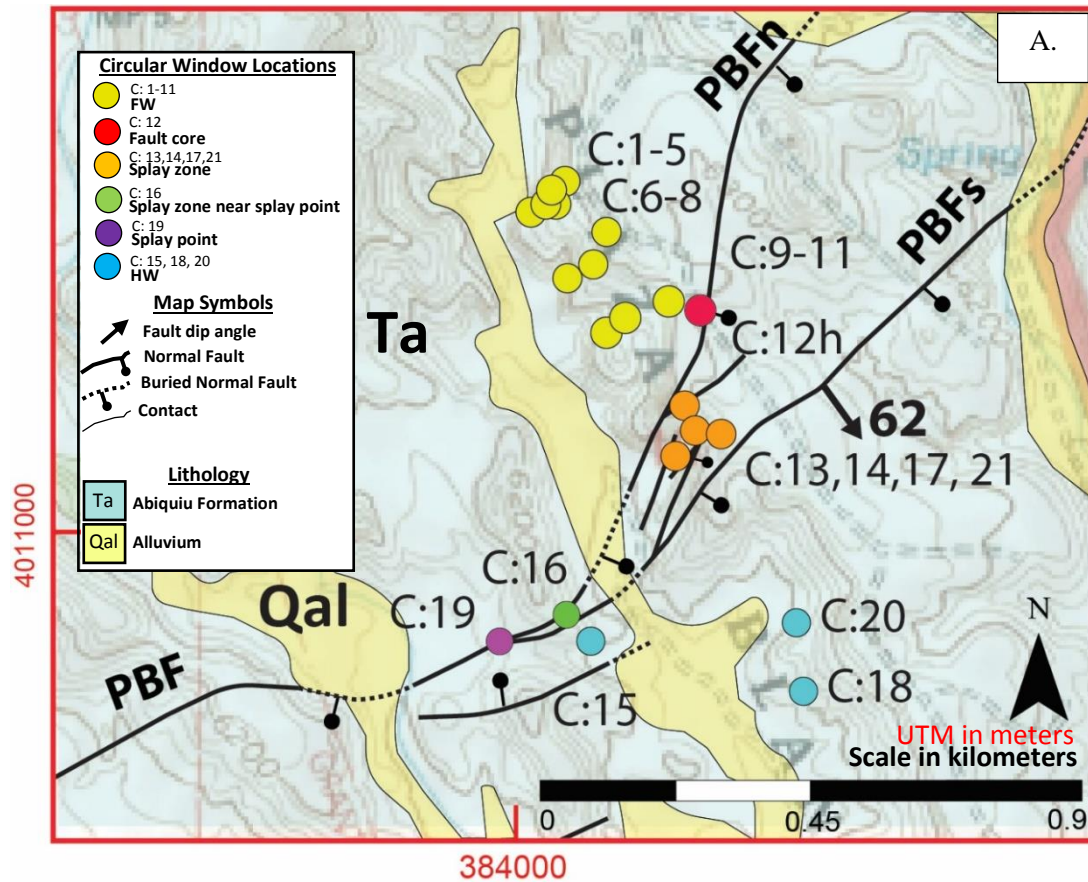


Figure 5.4.4: A. Geologic map of the Plaza Blanca Fault splay depicting fracture circle windows from the tactile fracture study. The circles are color coded to correspond with the circles on the ternary plot. B. A ternary diagram with I, X, Y end members showing connections per branch (C_B) defined by the equation and levels depicted by the dashed lines and represented numerically along the I-X side. The higher the C_B value the more connected a network is. Varying fracture network geometries exist and are typical with respect to location on the plot.

6. CONCLUSIONS

The methods used for characterizing fracture damage zones in the Plaza Blanca, New Mexico region yielded a data rich study. New concepts such as a “splay zone” are introduced to help explain a complex accommodation zone formed by a hard linked normal fault splay. Sampling techniques provided fracture information in three dimensions at various locations and at scales ranging from micrometer to kilometer. The following conclusions summarize the results of this study:

- The width of the damage zone at the Plaza Blanca fault is consistent with previous damage-zone width-versus-throw relationships.
- Fracture density in the damage zone increases with proximity to the fault core.
- Fracture density is highest at the fault core and splay point (branch line).
- The longer the fracture length, the more regularly oriented and similar to the regional features.
- The smaller fractures are more disordered and typically near the fault cores.
- Fracture density and connectivity have a positive quasi-linear relationship (Figure 6)
- The damage zone width across the Plaza Blanca Fault splay as it relates to throw is concordant with previous studies.
- The throw across the entire Plaza Blanca region exceeds that of the Cañones fault
- Microstructures at the fault cores depict cementation through fluid flow.
- Increased fracture density has the potential for increased permeability but shear fractures, grainsize reduction, and cementation may inhibit permeability rather than enhance it.

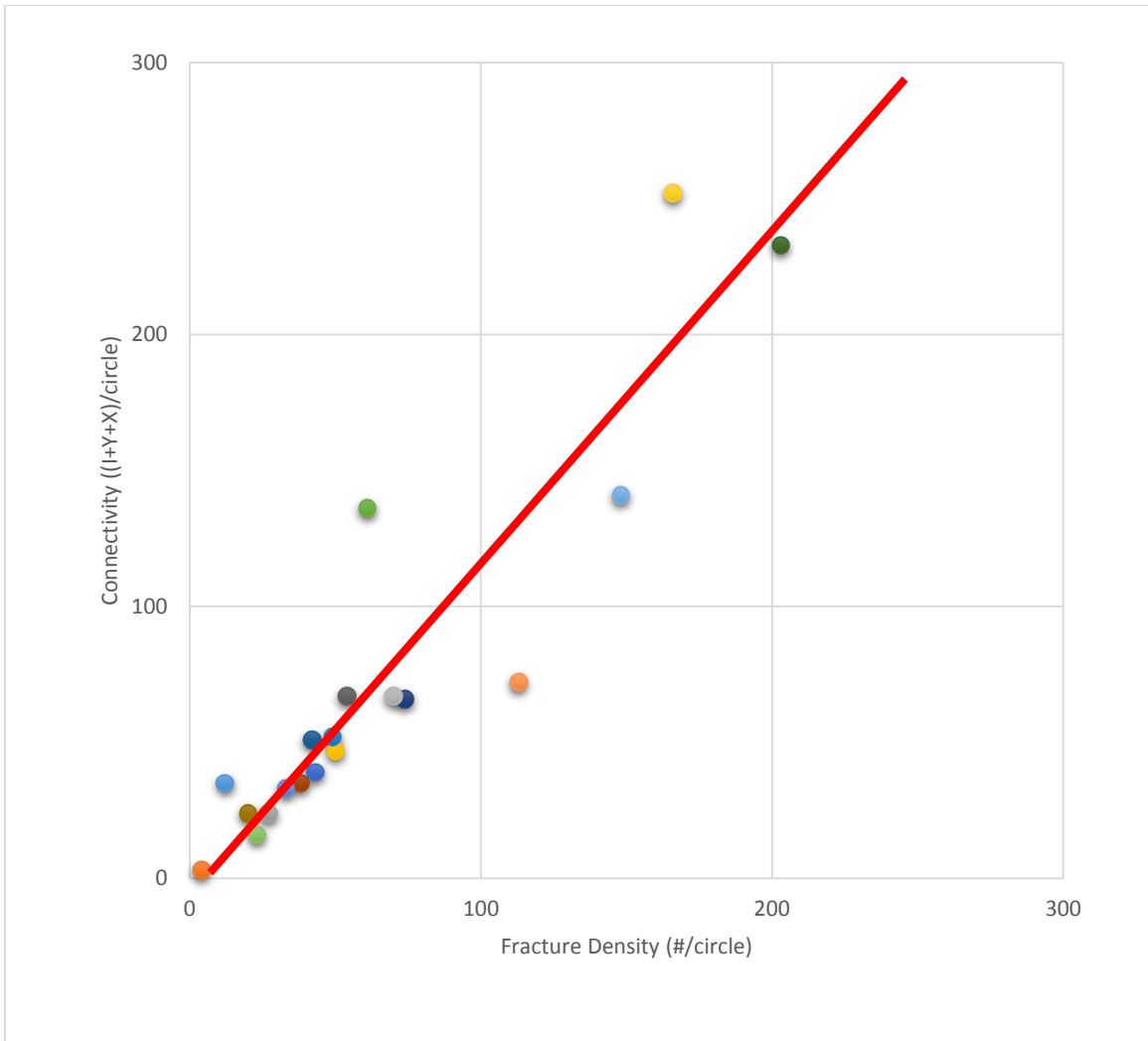
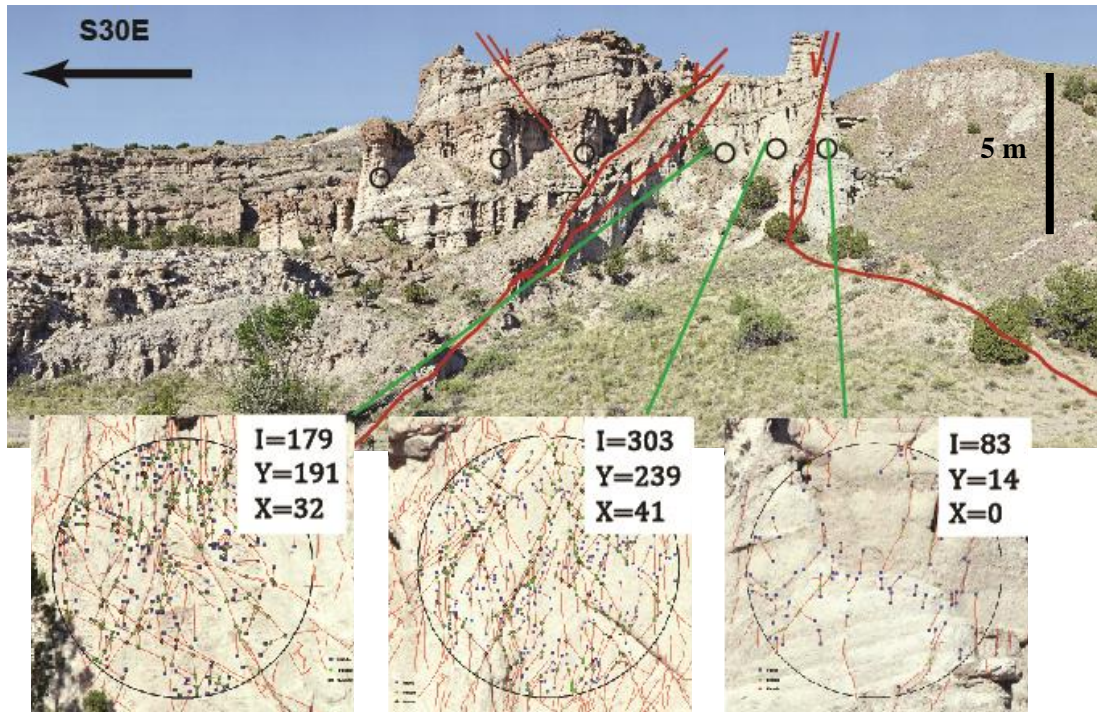


Figure 6: This is a graph showing the sum of connective facets per circle (I+X+Y) on the y-axis and the fracture density (number of fractures per circle area) on the x-axis. It shows a distinct positive quasi-linear relationship between connectivity and fracture density.

7. FUTURE WORK

The Plaza Blanca region is ripe with questions and outstanding hypothesis across many geologic disciplines. The following is a short list of future projects:

- Cerrito Blanca channel hypothesis needs some more field work.
- Understanding how groundwater is partitioned in the Abiquiu Formation requires some ground water well depth correlation.
- A compositional study of fracture fill using both hyperspectral imaging and thin section analysis can provide information about the type of cementation in the west splay zone of the Plaza Blanca region colloquially referred to as “Murphy’s Outcrop”.
- A continuation of fracture annotation of the other Gigapan in the Plaza Blanca Region can provide the foundation for a high resolution three dimensional view of the fracture damage zone.
- Applying the circular-window method and scan-line methods to Gigapan imagery can provide further information about detailed connectivity (see Figure 7).
- Detailed characterization of fracture mechanisms will provide further insight to transmissivity pathways for fluid. In this case groundwater.



Modified from Liu, Andrea, Murphy 2015

Figure 7: An annotated image of the Plaza Blanca fault splay looking southwest toward the converging faults approaching the splay point. The splay zone here is highly fractured and accommodates strain from two faults. The circular window method is applied to the Gigapan at more regular intervals along a single horizon for the purpose of topological connectivity characterization.

9. REFERENCES

- Anders M.H., Laubach S.E., Scholz C.H., 2014. Microfractures: A review. *Journal of Structural Geology*. 69, 377-394.
- Amato, J. M., Boullion, A. O., Serna, A. M., Sanders, A. E., Farmer, G. L., Gehrels, G. E., and Wooden, J. L. 2008. Evolution of the Mazatzal province and the timing of the Mazatzal orogeny: Insights from U-Pb geochronology and geochemistry of igneous and metasedimentary rocks in southern New Mexico. *Geological Society of America Bulletin*, 120(3-4), 328-346.
- Aronoff, R. F., Andronicos, C. L., Vervoort, J. D., and Hunter, R. A. (2016). Redefining the metamorphic history of the oldest rocks in the southern Rocky Mountains. *Geological Society of America Bulletin*, B31455-1.
- Baldrige, W.S., Damon, P.E., Shafiqullah, M., Bridwell, R.J., 1980. Evolution of the central Rio Grande rift, New Mexico: New potassium-argon ages. *Earth and Planetary Science Letters*. 51 (2), 309-321.
- Baldrige, W.S., Ferguson, J.F., Braile, L.W., Wang, B., Eckhardt, K., Evans, D., Schultz, C., Gilpin, B., Jiracek, G.R., and Biehler, S. (1994). The western margin of the Rio Grande Rift in northern New Mexico: An aborted boundary?. *Geological Society of America Bulletin*, 106(12), 1538-1551.
- Baldrige W.S., Keller G.R., Haak V., Wendlandt E., Jiracek G.R., Olsen K.H. 1995, The Rio Grande rift, in Olsen K.H. ed., *Continental Rifts: Evolution, Structure, and Tectonics*: Amsterdam, Elsevier Publishing, 233-275.
- Baldrige W.S., Olsen K.H. 1989. The Rio Grande Rift. *American Scientist*. 77, 240-247.
- Berglof, W. R. and McLemore, V. T., 2003, Economic geology of the Todilto Formation, New Mexico Geological Society, Guidebook, 54th Field Conference, Geology of the Zuni Plateau, p. 179-189.
- Billi, A., Francesco S., Fabrizio S., 2003. The damage zone-fault core transition in carbonate rocks: implications for fault growth, structure and permeability. *Journal of Structural Geology* 25, 1779-1794.
- Bird, P., 1988. Formation of the Rocky Mountains, western United States- A continuum computer model. *Science*, 239(4847), 1501-1507.
- Caine, J.S., Evans, J.P., Forster, C.B., 1996. Fault zone architecture and permeability structure. *Geology* 24 (11), 1025-1028.
- Cartwright J.A., Mansfield C.S., 1998. Lateral displacement variation and lateral tip geometry of normal faults in the Canyonlands National Park, Utah. *Journal of Structural Geology* 20 (1), 3-19.
- Cather, S. M., Chamberlin, R. M., Chapin, C. E., & McIntosh, W. C. 1994. Stratigraphic consequences of episodic extension in the Lemitar Mountains, central Rio Grande rift. *Geological Society of America Special Papers*, 291, 157-170.

- Cather, S.M., Karlstrom, K.E., Timmons, J.M., and Heizler, M.T., 2006, Palinspastic reconstruction of Proterozoic basement-related aeromagnetic features in north-central New Mexico: Implications for Mesoproterozoic to late Cenozoic tectonism: *Geosphere*, 2, 299-323.
- Chester J.S., Chester F.M., Kronenberg A.K., 2005. Fracture Surface energy of the Punchbowl fault, San Andreas system. *Nature* 437, 133-136.
- Childs, C., Manzocchi, T., Walsh, J.J., Bonson, C.G., Nicol, A., Schopfer, M.P.J., 2009. A geometric model of fault zone and fault rock thickness variations. *Journal of Structural Geology* 31 (2), 117-127.
- Church, F.S. and Hack, J.T., 1939. An Exhumed Erosion Surface in the Jemez Mountains, New Mexico. *The Journal of Geology* 47 (6), 613-629.
- Copeland, P., Currie, C. A., Lawton, T. F., & Murphy, M. A. (2017). Location, location, location: The variable lifespan of the Laramide orogeny. *Geology*, G38810-1.
- Currie J.B, Patnode H.W., Trump R.P., 1962. Development of Folds in Sedimentary Strata. *Geological Society of America Bulletin* 73, 655-674.
- Daniel, C. G., Pfeifer, L. S., Jones, J. V., and McFarlane, C. M. (2013). Detrital zircon evidence for non-Laurentian provenance, Mesoproterozoic (ca. 1490–1450 Ma) deposition and orogenesis in a reconstructed orogenic belt, northern New Mexico, USA: Defining the Picuris orogeny. *Geological Society of America Bulletin*, 125 (9-10), 1423-1441.
- Dawers N.H., Anders M.H., 1994. Displacement-length scaling and fault linkage. *Journal of Structural Geology* 17 (5), 607-614.
- Erslev, E. A. (2001). Multistage, multidirectional Tertiary shortening and compression in north-central New Mexico. *Geological Society of America Bulletin*, 113 (1), 63-74.
- Faulkner D.R., Jackson C.A.L., Lunn R.W., Schlische R.W., Shipton Z.K., Wibberley C.A.J., Withjack M.O., 2010. A review of recent developments concerning the structure, mechanics and fluid flow properties of fault zones. *Journal of Structural Geology* 32 (11), 1557-1575.
- Fossen, H., Johansen T.E.S., Hesthammer J., Rotevatn A., 2005. Fault interaction in porous sandstone and implications for reservoir management; examples from southern Utah. *AAPG Bulletin*, 89 (12), 1593–1606.
- Hudson, J. A., and J. P. Harrison, 1997. *Engineering rock mechanics: An introduction to the principles*: New York, Pergamon, 456 p.
- Hudson M.R., and Grauch V.J.S., 2013. Introduction. *GSA special papers*. 494, v-xii.
- Humphreys, E. D., 1995. Post-Laramide removal of the Farallon slab, western United States. *Geology*, 23(11), 987-990.
- Ingersoll RV, Cavazza W, Baldrige WS, Shafiqullah M. 1990. Cenozoic sedimentation and paleotectonics of north-central New Mexico: Implications for initiation and evolution of the Rio Grande rift. *Geological Society of America Bulletin* 102 (9), 1280-1296
- Ingersoll R.V. 2001. Structural and Stratigraphic Evolution of the Rio Grande Rift, Northern New Mexico and Southern Colorado. *International Geology Review*. 43, 867-891.

- Jamison W.R., Stearns D.W., 1982. Tectonic Deformation of Wingate Sandstone, Colorado National Monument. *AAPG Bulletin* 66 (12), 2584-2608.
- Karlstrom, K. E., Dallmeyer, R. D., and Grambling, J. A., 1997. $^{40}\text{Ar}/^{39}\text{Ar}$ evidence for 1.4 Ga regional metamorphism in New Mexico: Implications for thermal evolution of lithosphere in the southwestern USA. *The Journal of Geology*, 105(2), 205-224.
- Kellogg K.S. 1999, Neogene basins of the northern Rio Grande rift: partitioning and asymmetry inherited from Laramide and older uplifts: *Tectonophysics*, 305, 141-152.
- Kelley S.A., Osburn G.R., Ferguson C., Moore J., Kempter K., 2005. Geologic map of the Cañones quadrangle, Rio Arriba County, New Mexico DRAFT. New Mexico Bureau of Geology and Mineral Resources Open File Geologic Map.
- Kempter K., Kelley S., Zeigler K.E., Koning D.J., Lucas S. G., 2007. Geologic map of the Canjilon SE quadrangle, Rio Arriba County, New Mexico DRAFT. New Mexico Bureau of Geology and Mineral Resources Open File Geologic Map.
- Koning D.J., Kelley S., Zeigler K.E., Lucas S. G., 2006. Geologic map of the Ghost Ranch quadrangle, Rio Arriba County, New Mexico.,New Mexico DRAFT. New Mexico Bureau of Geology and Mineral Resources Open File Geologic Map.
- Koning D.J., Smith G.A., Aby S, 2008. Geologic map of the El Rito quadrangle, Rio Arriba County, New Mexico.New DRAFT. Mexico Bureau of Geology and Mineral Resources Open File Geologic Map.
- Kim, Y.S., Peacock, D.C.P., Sanderson, D.J., 2004. Fault damage zones. *Journal of Structural Geology* 26 (3), 503-517.
- Kluth, C. F. (1986). Plate tectonics of the Ancestral Rocky Mountains: Part III. Middle Rocky Mountains. *AAPG Memoir 41: Paleotectonics and Sedimentation in the Rocky Mountain Region, United States*. 353-369.
- Laubach S.E., Olson J.E., Gross M.R., 2009. Mechanical and fracture stratigraphy. *AAPG Bulletin*. 93(11), 1413–1426.
- Liu, L., Gurnis, M., Seton, M., Saleeby, J., Müller, R. D., Jackson, J. M., 2010. The role of oceanic plateau subduction in the Laramide orogeny. *Nature Geoscience*, 3(5), 353-357.
- Liu, Y., Murphy, M., O'Keeffe, K., Khadeeva, A., 2013. Oblique Extension and Basinward Tilting along the Cañones Fault Zone, West Margin of the Rio Grande Rift. *Geological Society of America Annual Meeting in Denver, Abstracts with Programs* 45 (7), 443.
- Liu, Y.A., Andrea, R.A., Murphy, M.A., 2015. Using topology to characterize fracture network in a normal fault splay zone in the Rio Grande rift, New Mexico. *GSA Annual Meeting, Baltimore, MD, Abstracts with Programs* 47(7), 510.
- Livaccari, R.F., 1991. Role of crustal thickening and extensional collapse in the tectonic evolution of the Sevier-Laramide orogeny, western United States. *Geology*, 19(11), 1104-1107.
- Lucas, S.G., 1993. The Chinle Group—Revised stratigraphy and biochronology of Upper Triassic strata in the western United States: *Museum of Northern Arizona Bulletin*, 59, 27–50.

- Maldonado, F., 2008. Geologic Map of the Abiquiu Quadrangle, Rio Arriba County, New Mexico. USGS.
- Mitchell T.M., Faulkner D.R., 2009. The nature and origin of off-fault damage surrounding strike-slip fault zones with a wide range of displacements: A field study from the Atacama fault system, northern Chile. *Journal of Structural Geology* 31 (8), 802–816.
- Maldonado, F., and Kelley, S.A., 2009, Revisions to the stratigraphic nomenclature of the Abiquiu Formation, Abiquiu and contiguous areas, north-central New Mexico: *New Mexico Geology*, 31, 3-8.
- Maldonado, F., Miggins, D. P., Budahn, J. R., and Spell, T., 2013. Deformational and erosional history for the Abiquiu and contiguous area, north-central New Mexico: Implications for formation of the Abiquiu embayment and a discussion of new geochronological and geochemical analysis. *Geological Society of America Special Papers*, 494, 125-155.
- Mitchell T.M., Faulkner D.R., 2012. Towards quantifying the matrix permeability of fault damage zones in low porosity rocks. *Earth and Planetary Science Letters* 339-340, 24-31.
- Morgan, P., Seager, W. R., & Golombek, M. P., 1986. Cenozoic thermal, mechanical and tectonic evolution of the Rio Grande rift. *Journal of Geophysical Research: Solid Earth*, 91(B6), 6263-6276.
- O’Keefe K.A., 2014. Geometry and kinematics of the Cañones Fault and the effects of lithology on the distribution of strain within the Cañones Fault damage zone. M.S. Thesis University of Houston.
- Okubo C.H., Schultz R.A., 2005. Evolution of damage zone geometry and intensity in porous sandstone: insight gained from strain energy density 162, 939-949.
- Peacock D.C.P., Sanderson D.J., 1994. Geometry and Development of Relay Ramps in Normal Fault Systems. *AAPG Bulletin* 78 (2), 147-165.
- Peacock D.C.P., 2002. Propagation, interaction and linkage in normal fault systems. *Earth-Science Reviews* 58 (1–2), 121–142.
- Rawling, G.C., Goodwin, L.B., Wilson, J.L., 2001. Internal architecture, permeability structure, and hydrologic significance of contrasting fault-zone types. *Geology* 29 (1), 43-46.
- Ricketts, J. W., Kelley, S. A., Karlstrom, K. E., Schmandt, B., Donahue, M. S., & van Wijk, J., 2016. Synchronous opening of the Rio Grande rift along its entire length at 25–10 Ma supported by apatite (U-Th)/He and fission-track thermochronology, and evaluation of possible driving mechanisms. *Geological Society of America Bulletin*, 128 (3-4), 397-424.
- Rohrbaugh Jr, M. B., Dunne, W. M., Mauldon, M., 2002. Estimating fracture trace intensity, density, and mean length using circular scan lines and windows. *AAPG Bulletin*, 86(12), 2089-2104.
- Sanderson, D.J. and Nixon, C.W., 2015. The use of topology in fracture network characterization. *Journal of Structural Geology*. 72, 55-66.

- Savage, H.M., Brodsky, 2011. E.E. Collateral damage: capturing slip delocalization in fracture profiles. *Journal of Geophysical Research*, submitted for publication. *Journal of Geophysical Research: Solid Earth* 116 (B3), doi: 10.1029/2010JB007665.
- Seager W.R., 2004. Laramide (Late Cretaceous-Eocene) tectonics of southwestern New Mexico, in Mack G.H., Giles K.A. eds., *The Geology of New Mexico, A Geologic History: New Mexico Geological Society Special Publication* 11, 183-202.
- Smith, T., Sundell, K., Johnston, S., Guilherme-Andrade, C., Andrea, R.A., Dickinson, J., Saylor, J., Liu, Y., Murphy, M., Lapen, T., *in prep.* Laramide tectonics, drainage dynamics, and basin development in north-central New Mexico.
- Shipton, Z.K. & Cowie, P.A., 2003. A conceptual model for the origin of fault damage zone structures in high-porosity sandstone. *Journal of Structural Geology*, 25, 333–345.
- Smith, H.T.U., 1938. Tertiary geology of the Abiquiu quadrangle, Rio Arriba County, New Mexico: *Journal of Geology*, 46, 933–965.
- Smith G.A., 1995. Paleogeographic, volcanologic and tectonic significance of the upper Abiquiu Formation at Arroyo del Cobre, New Mexico. *Geology of the Santa Fe Region. New Mexico Geological Society 46th Annual Fall Field Conference Guidebook*, 338 p.
- Ulmer-Scholle D.S., Scholle P.A., Schieber J., Raine R.J., 2014. *Memoir 109: A Color Guide to the Petrography of Sandstones, Siltstones, Shales and Associated Rocks. American Association of Petroleum Geologists. 507 p.*
- Watkins H., Butler R.W.H., Bond C.E., Healy D., 2015. Influence of structural position on fracture networks in the Torridon Group, Achnashellach fold and thrust belt, NW Scotland. *Journal of Structural Geology*. 74, 64–80.
- Walsh J.J., Manzocchi T., Nell P., Yielding G., 1999. Fault transmissibility multipliers for flow simulation models. *Petroleum Geoscience* 5(1), 53-63.
- Whitmeyer, S. J., and Karlstrom, K. E., 2007. Tectonic model for the Proterozoic growth of North America. *Geosphere*, 3(4), 220-259.
- Williams, M. L., 1991. Heterogeneous deformation in a ductile fold-thrust belt: The Proterozoic structural history of the Tusas Mountains, New Mexico. *Geological Society of America Bulletin*, 103(2), 171-188.
- Williams, M.L., Karlstrom, K.E., Lanzirrotti, A., Read, A.S., Bishop, J.L., Lombardi, C.E., Pedrick, J.N., and Wingsted, M. B., 1999. New Mexico middle-crustal cross sections. *Rocky Mountain Geology*, 34(1), 53-66.
- Vazzana, M.E., and Ingersoll, R.V., 1981, Stratigraphy, sedimentology, petrology, and basin evolution of the Abiquiu Formation (Oligo-Miocene), north-central New Mexico: Summary: *Geological Society of America Bulletin*, 92, 990-992.
- Ye, H., Royden, L., Burchfiel, C., and Schuepbach, M., 1996. Late Paleozoic deformation of interior North America: the greater Ancestral Rocky Mountains. *American Association of Petroleum Geologists Bulletin*, 80(9), 1397-1432.
- Yin, A., and Ingersoll, R.V., 1997. A model for evolution of Laramide axial basins in the southern Rocky Mountains, USA: *International Geology Review*, 39, 1113-1123.

Yonkee W.A. and Weil A.B., 2015. Tectonic evolution of the Sevier and Laramide belts within the North American Cordillera orogenic system. *Earth Science Reviews*, 150, 531-593.

Zahm C.K. and Hennings P.H., 2009. Complex Fracture Development related to stratigraphic architecture: Challenges for structural deformation prediction, Tensleep Sandstone at the Alcova antiline, Wyoming. *AAPG Bulletin*, 93, (11), 1427-1446.